Controlled drug delivery from iontophoretic systems

Miguel Silva Rente Antunes Cabrita

Controlled drug delivery from iontophoretic systems

Miguel Silva Rente Antunes Cabrita

Dissertation for the obtention of the Degree of **Master in Mathematics**

Area of Specialization in **Applied Analysis and Computation**

Oriented by **Professor José Augusto Ferreira**

Jury

President: Professor Maria Paula Oliveira

Members: Professor Gonçalo Pena

Professor José Augusto Ferreira

Date: 24 August 2015

Resumo

A modelação matemática é uma ferramenta poderosa que permite a representação virtual de fenómenos físicos e biológicos complexos e contribui para a compreensão do papel de cada sub fenómeno e da influência dos parâmetros do modelo no seu comportamento global. Para além disso, pode ser usada na construção de novos protocolos médicos, novos dispositivos para aplicação de fármacos e no planeamento de novas experiências e tratamentos.

Este trabalho é dedicado ao estudo da libertação controlada de fármacos a partir de dispositivos iontoforéticos. O transporte do fármaco e a sua absorção são favorecidos por campos elétricos. O fenómeno de libertação de fármaco é descrito por equações de convecção-difusão acopladas em que o coeficiente convectivo é definido pela equação de Nernst-Planck.

Iniciamos este trabalho com um modelo simplificado em que admitimos que o fármaco está em contacto com o tecido alvo. Neste caso, é estabelecida uma fórmula explícita para a concentração obtida utilizando a análise de Fourier. Na parte central do trabalho, o comportamento qualitativo do problema acoplado é analisado de um ponto de vista analítico e numérico. São estabelecidas estimativas de energia que nos permitem caracterizar a massa de fármaco absorvida. No ponto de vista numérico, é proposto um método de diferenças finitas e são estudadas as suas propriedades de estabilidade e convergência. Resultados numéricos que ilustram o comportamento qualitativo do sistema complexo são apresentados.

Palavras Chave: Libertação de fármacos, Iontoforese, Equação de Nernst-Plack, Equações de convecção-difusão acopladas

Abstract

Mathematical modelling is a powerful tool that allows a virtual representation of complex physical and biological phenomena and contributes to the understanding of the role of each phenomenon and the influence of the parameters of the model in its global behavior. Furthermore, it can be used to help the design of new protocols, new drug delivery devices and plan new experiments and treatments.

This work is devoted to the study of the controlled drug delivery from iontophoretic systems. The drug is entrapped in a reservoir which is in contact with a target tissue. The drug transport and its absorption are enhanced by an applied electric field. The drug release is described by coupled convection-diffusion equations, being the convective velocities given by the Nernst-Planck equation.

We start by considering a simplified model where the drug is in contact with the target tissue. In this case, an explicit expression for the drug concentration is obtained using Fourier analysis. In the main part of this work, the qualitative behavior of the coupled problems is analysed from theoretical and numerical points of view. Energy estimates are established that allow the characterization of the absorbed drug mass. From a numerical point of view, a finite difference method is proposed and its stability and convergence are established. Numerical results that illustrate the qualitative behavior of the drug concentration are included.

Keywords: Drug delivery, Iontophoresis, Nernst-Planck equation, Coupled convection-diffusion equations

Thank you note

I would first of all like to thank my family for always being supportive especially in the hardest times.

Thank you to my friends, in particular those who went through this journey with me this year: André Oliveira, Benvindo, and Levi. To Mafalda, for giving me crucial advice in a decisive moment, to João, for the peace he gave us by going across the Atlantic, and to Carolina, for the strength and belief she carried, when I lacked both. To Sílvia, Mário and André Gomes for the valuable company in study hours. Also, to all the friends Coimbra has given me, which could certainly not fit this page.

I would like to thank all the teachers I had throughout the years, who helped me build the knowledge I needed to complete this goal.

I must also say thank you, and apologize, to my jury, for the hours of torment they are about to endure, which I am certain they will pay back in kind.

Last but not least, to my supervisor Professor José Augusto Ferreira, with whom I learned immensely, I thank him for the time and patience he showed over the year.

Contents

Chapter 1

Introduction

Medical treatments using preparations for the skin, such as ointments and salves, are among the first to be recorded in medicine history. The transdermal route for drug delivery has since been one of the most used even today, mostly because of it's easy access and also for being potentially non-invasive. However, skin is foremost an important barrier in our defense system and, as such, constitutes an hindrance to most drugs by impeding the permeation and preventing them to reach the circulatory system in sufficient quantities.

To tackle this obstacle, several methodologies to increase skin permeation have been developed ([7]). Without being exhaustive, we mention: the use of chemical agents, even though an ideal chemical for penetration enhancement is hard to find; the sonophoresis, which uses ultrasound waves to stimulate micro-vibrations within the skin epidermis and creates a convective transport of the permeant across the skin; microneedles have also been used to bypass the stratum corneum (SC) through various techniques, such as coating the microneedles with the drug, or even using dissolvable microneedles with biodegradable polymeric materials ([15]) and letting the drug diffuse through the skin into the circulatory, after inserting them through the SC; the use of nanocarriers, the most used for transdermal drug delivery are liposomes, dendrimers, nanoparticles and nanoemulsions ([12]); and finally, a technique called iontophoresis, which consists in an application of a low electrical potential gradient over extended periods of time via an electrical circuit constituted by two oppositely charged drug reservoirs placed on the skin surface.

The last method, which is the object of this work, became popular at the beginning of the 20^{th} century through the work of LeDuc (1900). The electric field created enhances the flux or rate of absorption of ionic solutes into the skin. By alternately applying and terminating the current, one can have a greater control over the quantities of drug administered. A similar method called electroporation consists of applying a higher electrical potential gradient over shorter periods of time, which

"breaks" the cell membrane down and forms nano-scale defects or "pores" in the membrane ([1],[2], [3], [20]). Iontophoresis can be used in conjunction with electroporation and the previously refered methods. It should be remarked that iontophoresis is also applied to treat pancreatic cancer, using chemotherapy to shrink the tumor or to stop it's growth ([4]), therefore making some patients eligible to surgery which otherwise would not be. Ocular iontophoresis has been investigated to treatments such as dry eye syndrome. Dentistry has also recurred to iontophoretic uses in treating hypersensitive dentin, oral ulcers and delivering local anesthetics ([13]). Another important application regards the reverse iontophoresis, an alternative for non-invasive clinical and therapeutic drug monitoring ([7],[5]).

Some of the iontophoretic systems use stimuli-responsive polymers, where the drug is entrapped, that are able to respond to the modification of external environment like electric fields, pH, and temperature. Electric fields are an attractive stimulus because they can be precisely controlled, and the drug delivery responses can be predicted.

Each of the above applications involve complex phenomena. For instance, in transdermal drug delivery enhanced by an electric field, the drug leaves the polymeric matrix, enters the stratum corneum and is transported through the skin to reach the circulatory system. In both media the transport occurs by passive diffusion, electromigration-migration of ions due to the electric field, and electroosmosis-transport due the solvent movement ([10], [17], [19]).

Let us consider a coupled system: a reservoir containing a charged drug which is in contact with a target tissue. In iontophoresis procedure, a small electric field is applied to the coupled system. If the drug molecules are positively charged, then the anode is in contact with the reservoir and the cathode is in an opposite position. The generated electric field induces a convective field in the system that depends on the drug molecules' valence, intensity of the electric field, temperature, electric conductivity of both media and drug diffusion in the medium ([10],[11]).

Mathematical modelling is a powerful tool that allows a virtual representation of the physical and biological phenomena involved and contributes to the understanding of the role of each phenomenon, the influence of the parameters of the model in its global behavior and to justify experimental data. Furthermore, it can be used to help the design of new protocols, new drug delivery devices and plan new experiments and treatments.

The main objective of this work is the mathematical modelling of the drug released from a polymeric matrix and its entrance in a target tissue when the iontophoresis procedure is used. In this case, the drug delivery from a polymeric device is enhanced by an electric field of low intensity, which is applied during long periods of time, and its entrance in a target tissue is also enhanced by the electric field. The mathematical model is characterized by partial differential equations that describe the transport through the media-polymeric matrix and target tissue, and the evolution of the electric field which is described by the Laplace equation in both media. The electric potential induces a convective field that enhances the drug transport. Then, the time-space evolution of the drug in both media is described by convection-diffusion equations and additional conditions: initial, boundary and interface conditions ([11]).

This work is organized as follows. In Chapter 2 we consider the case in which the drug is in direct contact with the target tissue, with an electrode inside the target. An analytical study is presented regarding existence and uniqueness of a solution of the convection-diffusion equation, and the obtained solution is illustrated. In Chapter 3 the more complex case of a drug encapsulated in a reservoir is studied. Solving the coupled problem for the electric field, the convective field is explicitly given and the electric field and drug equations are replaced by coupled convection-diffusion equations. Energy estimates are obtained and used to guarantee the uniqueness and stability of the coupled model, as well as to compute lower bounds for the absorbed drug. As we are not able to obtain an explicit expression for the drug concentration, we introduce an explicit Euler method, that allow us to compute an approximation for the solution. The stability and convergence of the proposed numerical method are presented. Some numerical results obtained with *Matlab* are also included. We observe that part of these studies were published in [8]. In Chapter 4 we present some conclusions.

Chapter 2

Drug in contact with the target tissue

2.1. Introduction

The main objective of this Chapter is the study of the situation when the drug is constantly being delivered directly to the target tissue. To enhance the drug diffusion, we assume that an electric field is applied. In this case the drug mass flux J has two main contributes: the Fick's mass flux and a convective mass flux induced by the electric field. Here we shall neglect the osmotic mass flux and assume that the target tissue is an isotropic medium. This last assumption allow the replacement of the 3D model by a 1D model. The iontophoretic device is considered with the anode and cathode placed in the intended direction of the drug and opposite to each other, with one being implanted in the intended target. This can be the case as in the administration of cytotoxic therapies ([4]). This Chapter is organized as follows: in Section 2.2 we present the evolution of the drug concentration. The construction of the solution of the initial value problem introduced in the previous Section is made using the method of separation of variables in Section 2.3. This construction allows us to illustrate the drug concentration behavior in Section 2.4 and the response to the changes of some parameters.

2.2. Evolution of the drug concentration

Let $c(x,t)$ (g/m^3) represent the drug concentration in $x \in [0,\ell]$ at time $t \geq 0$. In $x = 0$ we have the point of contact between the drug and the tissue and in $x = \ell$ the point of desired absorption as in figure 2.1. Consider c_{ext} to be the concentration of drug molecules at $x = 0$. At the initial time $t = 0$ we do not have any drug in the tissue and we assume that the drug is completely absorbed at $x = \ell$. These assumptions can be summarized by

$$c(0,t) = c_{ext}\,,\ t \geq 0\,, \qquad c(\ell,t) = 0\,,\ t \geq 0\,, \qquad c(x,0) = 0\,,\ x \in (0,\ell)\,. \tag{2.1}$$

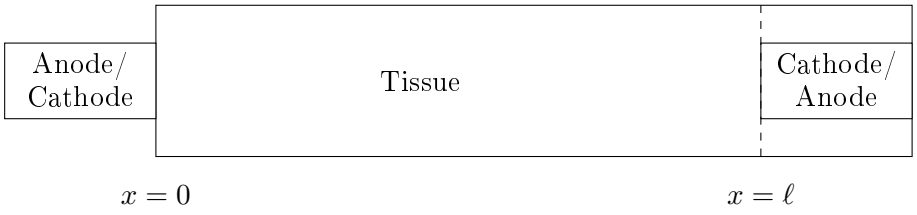

Figure 2.1: Considered model.

The drug mass flux ($g\,m^{-2}\,s^{-1}$) is given by the Nernst-Planck equation

$$J = -D\nabla c - vc\,, \tag{2.2}$$

where D ($m^2\,s^{-1}$) is the diffusion coefficient and v the convection velocity induced by the applied electric field

$$v = \frac{zDF}{RT}\nabla\Phi \tag{2.3}$$

where z denotes the valence of the drug molecules, F the Faraday constant ($9.6485 \times 10^4\, Coulomb/mol$), T the temperature (K) in the tissue, R the gas constant ($8.31446\ JK^{-1}mol^{-1}$) and Φ (V) the electric potential.

The mass conservation law dictates

$$\frac{\partial c}{\partial t} + \nabla \cdot J = 0, \tag{2.4}$$

and from (2.2) we obtain

$$\frac{\partial c}{\partial t} = \nabla \cdot (D\nabla c) + \nabla \cdot (vc)\,. \tag{2.5}$$

Next we shall compute the gradient of the potential. We assume that during the period of application, Φ does not change over time. Then

$$\Delta\Phi = 0\,,\ \text{in}\ (0,\ell)\,. \tag{2.6}$$

Since the applied potential is known,

$$\Phi(0) = \Phi_0 \qquad \Phi(\ell) = \Phi_1\,, \tag{2.7}$$

we obtain

$$v = \frac{zDF}{RT}\frac{\Phi_1 - \Phi_0}{\ell}\,. \tag{2.8}$$

Regarding the ionic valance z and the potential difference $\nabla\Phi$, we make the following observation. If the ionic specie has a positive electric charge, one needs to generate a potential difference by placing the anode in the left-hand side of the

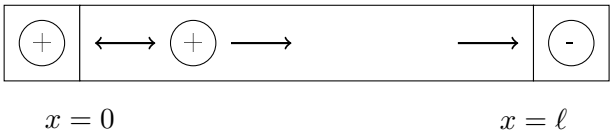

Figure 2.2: Scheme for a positively charged drug.

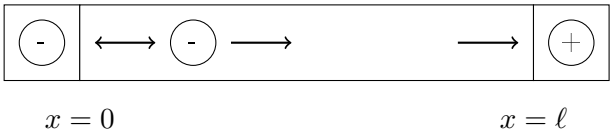

Figure 2.3: Scheme for a negatively charged drug.

target tissue and the cathode in the opposite side. In figure 2.3 we illustrate the converse situation for a negative ionic valence.

Finally we conclude from (2.5) and (2.1), and considering the 1D simplification, that the evolution of the drug concentration is described by the following initial and boundary value problem

$$\begin{cases} \dfrac{\partial c}{\partial t} = D\dfrac{\partial^2 c}{\partial x^2} + \dfrac{\partial}{\partial x}(vc) & \text{in } (0,\ell)\times\mathbb{R}^+ \\ c(x,0) = 0, & x \in (0,\ell) \\ c(0,t) = c_{ext}\,, \quad c(\ell,t) = 0, & t \in \mathbb{R}_0^+ \end{cases} . \tag{2.9}$$

2.3. Existence and uniqueness results

In what follows we will study the existence and uniqueness of the solution of the IBVP (2.9). We start our analysis by assuming that solutions for this problem exist and we will prove the uniqueness of such a solution.

Theorem 1. *The IBVP (2.9) has at the most one solution* $c(t) \in \mathbb{H}^2(\Omega)$ *and* $\dfrac{\partial c}{\partial t}(t) \in \mathbb{L}^2(\Omega)$.

We shall use the following notations: for $t \in \mathbb{R}_0^+$, by $c(t)$ we denote the function

$$\begin{aligned} c(t)\colon [0,\ell] &\to \mathbb{R} \\ x &\mapsto c(x,t). \end{aligned}$$

Let $\mathbb{L}^2(0,\ell)$ be the usual space of square integrable functions with the usual inner product $(\ ,\ )$ and norm $\|\ .\ \|$. By $\mathbb{H}^1(0,\ell)$, $\mathbb{H}_0^1(0,\ell)$ we represent the usual Sobolev spaces.

Suppose that c satisfies the Dirichlet homogenous boundary conditions and the initial condition holds as stated in (2.9). Then, from (2.5) we obtain

$$(c'(t), w) + (D\nabla c(t), \nabla w) + (\nabla vc, \nabla w) = 0\,,\ \forall w \in \mathbb{H}^2(0,\ell) \tag{2.10}$$

If (2.9) has two solutions c_1 and c_2, then $c = c_1 - c_2$ satisfies (2.10). Consequently, taking $w = c$ we get

$$\frac{1}{2}\frac{d}{dt}||c(t)||^2 + D||\nabla c(t)||^2 + (vc(t), \nabla c(t)) = 0$$

and since

$$(vc(t), \nabla c(t)) \leq \frac{v^2}{4\varepsilon^2}||c(t)||^2 + \varepsilon^2||\nabla c(t)||^2$$

$\forall \varepsilon \in \mathbb{R}\setminus\{0\}$, we obtain

$$\frac{1}{2}\frac{d}{dt}||c(t)||^2 + (D - \varepsilon^2)||\nabla c(t)||^2 - \frac{v^2}{4\varepsilon^2}||c(t)||^2 \leq 0\,. \tag{2.11}$$

Choosing $\varepsilon^2 = D$ we establish

$$\frac{1}{2}\frac{d}{dt}||c(t)||^2 - \frac{v^2}{4D}||c(t)||^2 \leq 0\,,\ \forall t > 0\,. \tag{2.12}$$

Gronwall's lemma allow us to obtain the following estimate

$$||c(t)||^2 \leq e^{\frac{v^2}{4D}t}||c(0)||^2\,,\ \forall t \geq 0\,. \tag{2.13}$$

Inequality 2.13 leads to the uniqueness of the solution of the IBVP (2.9) and its stability. In fact, if c_1 and c_2 are both solutions of (2.9) with different initial conditions, then

$$||c_1(t) - c_2(t)||^2 \leq e^{\frac{v^2}{4D}t}||c_1(0) - c_2(0)||^2\,,\ \forall t > 0\,. \tag{2.14}$$

Consequently, we conclude that we have stability, but only in bounded time intervals.

Let us now show that a solution of the problem exists.

Theorem 2. *The function* $c(x,t) = \frac{\ell - x}{\ell}c_{ext} + e^{\alpha x + \beta t}\sum_{n=0}^{+\infty} a_n(t) sin(\frac{n\pi x}{\ell})$, $(x,t) \in [0,\ell] \times \mathbb{R}_0^+$ *with*

- $a_n(t) = B_n \dfrac{e^{-\beta t} - e^{-d(\frac{n\pi}{\ell})^2 t}}{d(\frac{n\pi}{\ell})^2 - \beta} + e^{-d(\frac{n\pi}{\ell})^2 t}a_n(0)\,,$
- $a_n(0) = -\dfrac{2c_{ext}}{\ell}\dfrac{e^{-\alpha\ell}\ell(e^{\alpha\ell}n\pi(\alpha\ell(-2+\alpha\ell) + n^2\pi^2) - 2\alpha\ell n\pi\cos(n\pi)}{((\alpha\ell)^2 + (n\pi)^2)^2}$
- $B_n = \dfrac{2vc_{ext}}{\ell^2}\left(\dfrac{n\pi\ell(1 - e^{\alpha\ell}\cos(n\pi)}{(n\pi)^2 + (\alpha\ell)^2}\right)\,,$

- $\alpha = -\frac{v}{2D}$ *and* $\beta = -\frac{v^2}{4D}$,

satisfies the convection-diffusion equation (2.9) and the initial conditions in the sense that the boundary conditions hold.

Proof. We start by reducing the boundary condition to a homogenous boundary condition considering $w = c - w_0$, where

$$w_0(x) = \frac{\ell - x}{\ell} c_{ext}\,.$$

As we have

$$\begin{aligned}\frac{\partial w}{\partial t} &= \frac{\partial c}{\partial t} - \frac{\partial w_0}{\partial t} = \frac{\partial c}{\partial t} \\ &= D\frac{\partial^2 c}{\partial x^2} + \frac{\partial}{\partial x}(vc) \\ &= D\frac{\partial^2 w}{\partial x^2} + \frac{\partial}{\partial x}(vw) + \frac{v}{\ell} c_{ext}\,,\end{aligned}$$

we conclude for w

$$\begin{cases} \frac{\partial w}{\partial t} = D\frac{\partial^2 w}{\partial x^2} + \frac{\partial}{\partial x}(vw) + \frac{v}{\ell} c_{ext} & \text{in } (0,\ell)\times\mathbb{R}^+ \\ w(x,0) = -\frac{\ell - x}{\ell} c_{ext}\,, & x \in (0,\ell) \\ w(0,t) = 0\,, \quad w(\ell,t) = 0\,, & t \in \mathbb{R}^+ \end{cases} . \tag{2.15}$$

To remove the term $\frac{\partial}{\partial x}(vw)$ we introduce the new variable $w(x,t) = e^{\alpha x + \beta t} g(x,t)$, where α and β will be fixed later. Then we have

$$\begin{aligned}\frac{\partial w}{\partial t}(x,t) &= \beta e^{\alpha x+\beta t} g(x,t) + e^{\alpha x+\beta t}\frac{\partial g}{\partial t}(x,t) \\ \frac{\partial w}{\partial x}(x,t) &= \alpha e^{\alpha x+\beta t} g(x,t) + e^{\alpha x+\beta t} \\ \frac{\partial^2 w}{\partial x^2}(x,t) &= \alpha^2 e^{\alpha x+\beta t} g(x,t) + 2\alpha e^{\alpha x+\beta t}\frac{\partial g}{\partial x}(x,t) + e^{\alpha x+\beta t}\frac{\partial^2 g}{\partial x^2}(x,t)\,.\end{aligned}$$

From equations (2.15) and dividing by $e^{\alpha x+\beta t}$ on both sides we obtain

$$\frac{\partial g}{\partial t}(x,t) = g(x,t)\left(D\alpha^2 + v\alpha - \beta\right) + \frac{\partial g}{\partial x}(x,t)(2\alpha D + v) + \frac{\partial^2 g}{\partial x^2}(x,t)D + \frac{v}{\ell} c_{ext} e^{-\alpha x - \beta t}\,.$$

Fixing $\alpha = -\frac{v}{2D}$ and $\beta = -\frac{v^2}{4D}$ we get for g the following IBVP

$$\begin{cases} \frac{\partial g}{\partial t}(x,t) = D\frac{\partial^2 g}{\partial x^2}(x,t) + \frac{v}{\ell} c_{ext} e^{-\alpha x - \beta t}\,, & (x,t) \in (0,\ell)\times\mathbb{R}^+ \\ g(x,0) = -\frac{\ell - x}{\ell} c_{ext} e^{-\alpha x}\,, & x \in (0,\ell) \\ g(0,t) = 0\,, \quad g(\ell,t) = 0\,, & t \in \mathbb{R}^+ \end{cases} . \tag{2.16}$$

We prescribe for the solution of (2.16) the following form

$$g(x,t) = \sum_{n=1}^{+\infty} a_n(t) \sin\left(\frac{n\pi x}{\ell}\right) . \tag{2.17}$$

Let $f(x,t) = \frac{v}{\ell} c_{ext} e^{-\alpha x - \beta t}$. Then $f(x,t) = e^{-\beta t} f(x)$ where

$$f(x) = \sum_{n=1}^{+\infty} B_n \sin\left(\frac{n\pi x}{\ell}\right)$$

and B_n, the Fourier coefficients of $f(x)$, are given by

$$B_n = \frac{2vc_{ext}}{\ell} \left(\frac{n\pi(1 - e^{-\alpha\ell}\cos(n\pi)}{(n\pi)^2 + (\alpha\ell)^2} \right) .$$

We establish in what follows, a differential equation for the Fourier coefficients $a_n(t)$. We have

$$\frac{\partial g}{\partial t}(x,t) = \sum_{n=1}^{+\infty} a_n'(t) \sin\left(\frac{n\pi x}{\ell}\right) .$$

From the differential equation for g we deduce

$$\sum_{n=1}^{+\infty} a_n'(t) \sin\left(\frac{n\pi x}{\ell}\right) = -D \sum_{n=1}^{+\infty} a_n(t) \left(\frac{n\pi x}{\ell}\right)^2 \sin\left(\frac{n\pi x}{\ell}\right) + e^{-\beta t} \sum_{n=1}^{+\infty} B_n \sin\left(\frac{n\pi x}{\ell}\right) .$$

Therefore, we are led to the following differential equation

$$a_n'(t) = -D \left(\frac{n\pi x}{\ell}\right)^2 a_n(t) + e^{-\beta t} B_n \tag{2.18}$$

which is complemented by the Fourier coefficients of $g(x,0)$ given by

$$a_n(0) = -\frac{2c_{ext}}{\ell} \frac{e^{-\alpha\ell}\ell(e^{\alpha\ell} n\pi(\alpha\ell(-2+\alpha\ell) + n^2\pi^2) + 2\alpha n\ell\pi\cos(n\pi))}{((\alpha\ell)^2 + (n\pi)^2)^2} . \tag{2.19}$$

Solving the initial value problem (2.18), (2.19) we obtain

$$a_n(t) = B_n \frac{e^{-\beta t} - e^{-d(\frac{n\pi}{\ell})^2 t}}{d(\frac{n\pi}{\ell})^2 - \beta} + e^{-d(\frac{n\pi}{\ell})^2 t} a_n(0) .$$

Since $w = c - w_0$, then

$$c(x,t) = w(x,t) + w_0(x) = e^{\alpha x + \beta t} g(x,t) + w_0(x) ,$$

that is,

$$c(x,t) = \frac{\ell - x}{\ell} c_{ext} + e^{\alpha x + \beta t} \sum_{n=1}^{+\infty} a_n(t) \sin\left(\frac{n\pi x}{\ell}\right) , \ x \in [0,\ell] , \ t \geq 0 . \tag{2.20}$$

It remains to check if c is indeed a solution of the IBVP. We prove in what follows that $g(x,t)$ exists for $x \in [0,\ell]$, $t \geq 0$, that is, the series in the right-hand side of (2.20) is uniformly convergent in $[0,\ell] \times [\gamma, T]$ for $\gamma > 0$, $\gamma < T$ and a fixed T.

We remark that for $x \in [0,\ell] \times [\gamma, T]$ we have

$$\left|a_n(t)\sin\left(\frac{n\pi x}{\ell}\right)\right| \leq const\left[\left(\frac{n}{n^2+\alpha'}\right)\left(\frac{1}{n^2-\beta'}\right) + e^{-d\left(\frac{n^2\pi^2}{\ell}\right)}\left(\frac{n^3+n}{(\hat{\alpha}+n^2)^2}\right)\right]$$

for convenient constants α', $\hat{\alpha}$, β' and for $n \geq n_0$ such that $n^2 - \beta' > 0$. In the last inequality and in what follows we denote *const* also a convenient constant.

As $\sum_{n=n_0}^{+\infty} \frac{n}{(n^2+\alpha')(n^2-\beta')}$ and $\sum_{n=n_0}^{+\infty} e^{-d\left(\frac{n^2\pi^2}{\ell}\right)} \frac{n^3+n}{(\hat{\alpha}+n^2)^2}$ are convergent series, we conclude that $\sum_{n=1}^{+\infty} a_n(t)\sin\left(\frac{n\pi x}{\ell}\right)$ is uniformly convergent in $[0,\ell] \times [\gamma, T]$ and so, it defines a continuous function in $[0,\ell] \times [\gamma, T]$. Finally, we conclude that g exists and is continuous in $[0,\ell] \times \mathbb{R}^+$.

Following the previous procedure for

$$\sum_{n=1}^{+\infty} a_n^{(i)}(t)\left(\frac{d}{dx}\right)^j \sin\left(\frac{n\pi x}{\ell}\right) \ , x \in (0,\ell\,,\ t \in [\gamma, T]\,,$$

it can be shown that $\dfrac{\partial^{i+j} g}{\partial x^i \partial t^j}$ exists and is continuous in $(0,\ell) \times \mathbb{R}^+$.

By the construction of the ordinary differential problem for $a_n(t)$, it is easy to conclude that g satisfies the differential equation of the IBVP (2.16).

We will now prove that g satisfies the initial condition in (2.16) in the sense that (2.16) holds. Let $\Psi \in \mathbb{L}^2(0,\ell)$. We have

$$\begin{aligned}\lim_{t\to 0^+}(g(t),\Psi) &= \lim_{t\to 0^+}\sum_{n=1}^{+\infty} a_n(t)\int_0^\ell \Psi(x)\sin\left(\frac{n\pi x}{\ell}\right)\mathrm{d}x \\ &= \lim_{t\to 0^+}\frac{\ell}{2}\sum_{n=1}^{+\infty} a_n(t)b_n\,.\end{aligned}$$

We show now that $\sum_{n=1}^{+\infty} a_n(t)b_n$ is a continuous function for $t \geq 0$. We have

$$|a_n(t)b_n| \leq const\left(\frac{n}{n^2+\alpha'}\frac{1}{n^2-\beta'} + \frac{n^3+n}{(\hat{\alpha}+n^2)^2}\right)|b_n|$$

for $t \geq 0$ and $n \geq n_0$. Consequently

$$\begin{aligned}\sum_{n=n_0}^{m}|a_n(t)b_n| &\leq const\sum_{n=n_0}^{m}\left(\frac{n}{n^2+\alpha'}\frac{1}{n^2-\beta'} + \frac{n^3}{(\hat{\alpha}+n^2)^2}\right)|b_n| \\ &\leq const\left(\sum_{n=n_0}^{m}\frac{n^2}{(n^2+\alpha')^2(n^2-\beta')^2} + \frac{n^6}{(\hat{\alpha}+n^2)^4}\right)^{\frac{1}{2}}\left(\sum_{n=n_0}^{m}|b_n|^2\right)^{\frac{1}{2}}.\end{aligned}$$

As $\sum_{n=n_0}^{m}\frac{n^2}{(n^2+\alpha)^2(n^2-\beta)^2}$ and $\sum_{n=n_0}^{m}\frac{n^3}{(\alpha+n^2)^4}$ are convergent sequences because the corresponding series are convergent, and $\sum_{n=n_0}^{m}|b_n|^2$ is convergent because $\Psi \in \mathbb{L}^2(0,\ell)$, then $\sum_{n=1}^{+\infty}|a_n(t)b_n|$ is convergent for $t \geq 0$, and consequently $\sum_{n=1}^{+\infty} a_n(t)b_n$ is a continuous function for $t \geq 0$.

Using the previous property, we have

$$\begin{aligned}\lim_{t\to 0^+}(g(t),\Psi) &= \frac{\ell}{2}\sum_{n=1}^{+\infty} a_n(0)b_n \\ &= (g(0),\Psi)\,.\end{aligned}$$

□

2.4. Qualitative behavior

In Theorem 2 we have presented an explicit expression for the drug concentration c using a Fourier series. Considering a finite number of terms of such series, we obtain an approximation for c. Here we shall consider $N = 2000$, that is

$$c_{2000}(x,t) = \frac{\ell - x}{\ell}c_{ext} + e^{\alpha x+\beta t}\sum_{n=1}^{2000} a_n(t)\sin\left(\frac{n\pi x}{\ell}\right)\,.$$

In what follows we illustrate the behavior of c_{2000} for different values of the parameters of the model. We start by illustrating the effect of the convection term, induced by the electric field. We have taken $c_{ext} = 1$ (g/m^2), $D = 10^{-11}$ (m^2/s), $\ell = 1.13\times 10^{-3}$ m and $z = -1$. On figure 2.4 we present $c_{2000}(t)$ for different values of t and with $v = 0$, a diffusion process. In figure 2.5 we present the concentration c_{2000} when electromigration is present, with $\Phi_0 = -0.02$ V and $\Phi_1 = 0.02$ V. We observe an increase in concentration levels in the last case, when compared to only diffusion illustrated in figure 2.4.

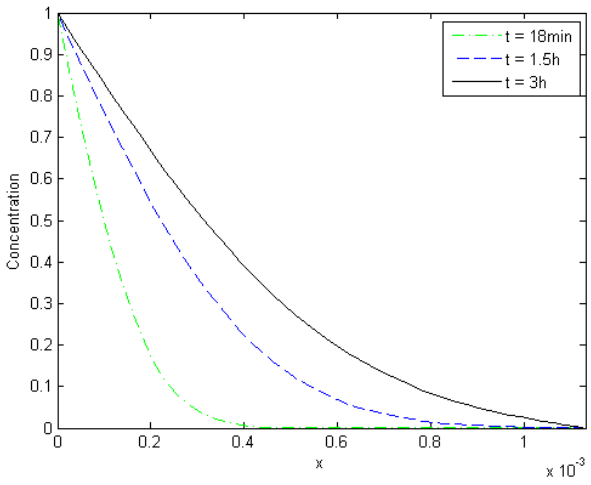

Figure 2.4: Evolution of the concentration between 3 hours with just diffusion.

In figure 2.6 we illustrate the effect of the electric potential. In this figure we plot the drug concentration c_{2000}, using the same value for $D = 10^{-11}$, with different

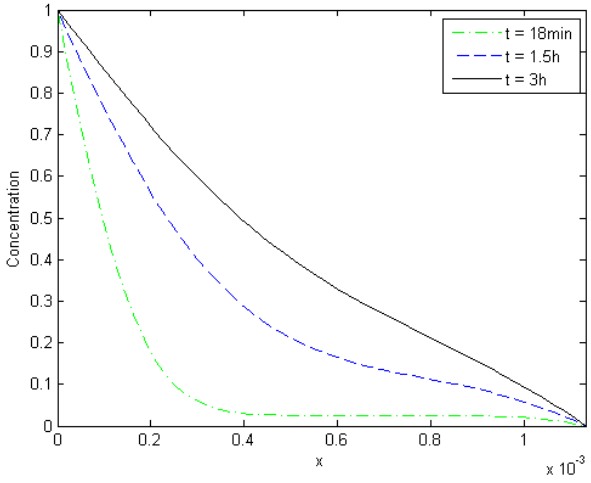

Figure 2.5: Evolution of the concentration between 3 hours with electromigration.

$\ell\nabla\Phi = 0.02$, 0.04 and 0.08, after the same time $t = 3\ h$. We observe that as $\ell\nabla\Phi$ increases, higher values of concentration are obtained.

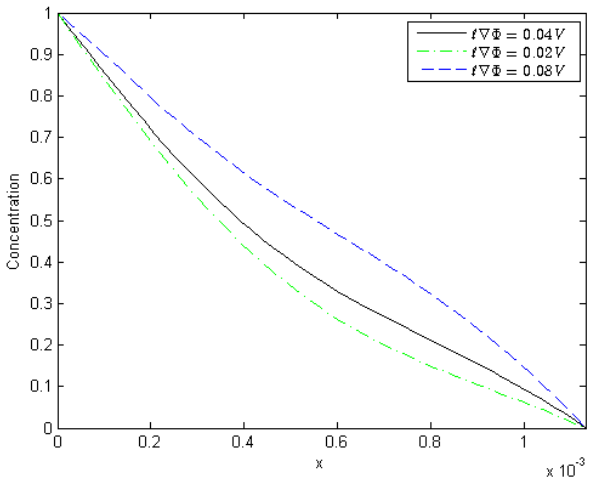

Figure 2.6: Concentration after 3 hours with different potentials.

The effect of the diffusion coefficient in the transport process is illustrated in figure 2.7, where we use for the same $\Phi_0 = -0.02$ and $\Phi_1 = 0.02$, different values of $D = 10^{-11}$, 2×10^{-12} and 5×10^{-11}.

As we can see, small increases in the potential and the diffusion coefficient lead to a general increase of the concentration after some time, whereas small decreases lead to a decrease of the concentration.

We will now turn our attention towards the stationary solution of the problem.

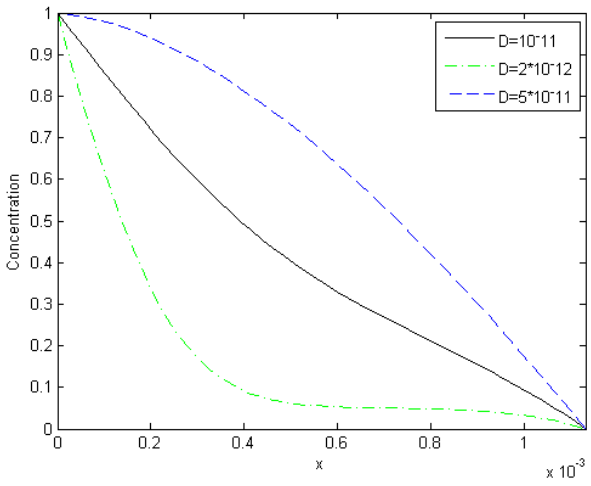

Figure 2.7: Concentration after 3 hours with different diffusion coefficients.

Solving $\frac{\partial c}{\partial t} = 0$ we obtain

$$c(x) = \frac{c_{ext}}{1 - e^{\frac{v*\ell}{D}}} \left(e^{\frac{v}{D}x} - e^{\frac{v*\ell}{D}} \right), \; x \in [0, \ell] \, .$$

Note that, from the expression for v in (2.8), the electric potential can influence the stationary solution. In fact, we can see that a higher electrical potential leads to higher stationary concentration levels. Furthermore, observing the expression for v we can say that the diffusion coefficient does not influence the stationary state. In figures 2.8 and 2.9 we plot the stationary solutions for $\ell \nabla \Phi = 0$ and $\ell \nabla \Phi = 0.04$ respectively.

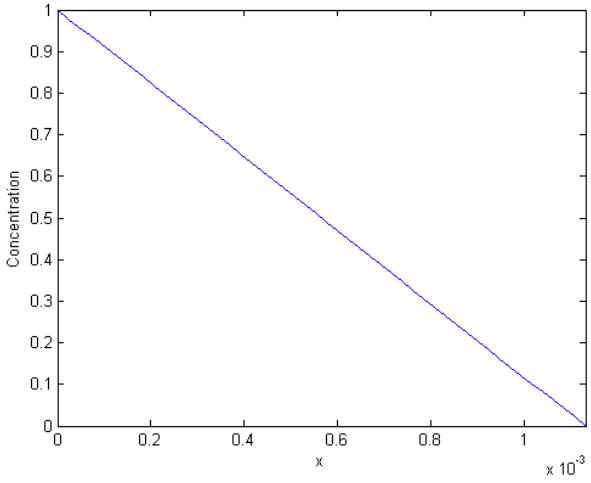

Figure 2.8: Stationary state of concentration with $\ell \nabla \Phi = 0$.

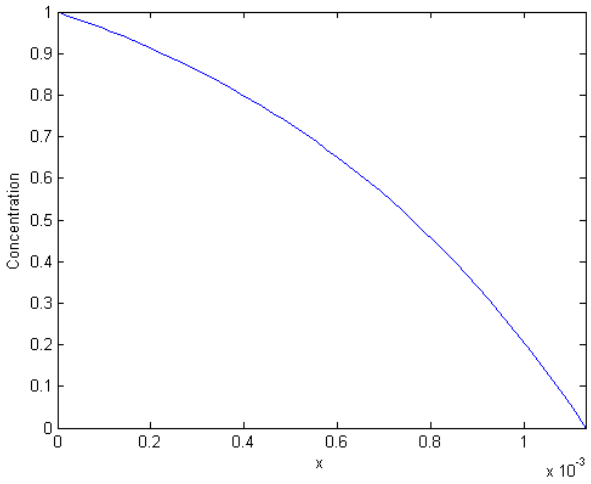

Figure 2.9: Stationary state of concentration with $\ell \nabla \Phi = 0.04$.

Chapter 3

Drug in a polymeric reservoir

3.1. Introduction

In this Chapter we assume that the drug is contained in a polymeric reservoir which is in contact with the target tissue. The electric field is generated applying the cathode (anode) in the reservoir and the anode (cathode) in the oposite site, in the target tissue depending on the electric charge of the drug as it was observed in Chapter 2. Since we assume isotropic media, the 3D physical model can be replaced by a 1D physical model as the one illustrated in figure 3.1. As the drug transport in the reservoir and in the target tissue is enhanced by the electric field, the drug mass flux J_i, $i = r, s$, has two main contributions, which are induced by the Fickian transport and electromigration as in Chapter 2. We assume that the two media have different diffusion and electrical conductivity coefficients. These assumptions lead to two different Laplace equations for the electric potential that are coupled by transference conditions at the contact boundary. The evolution of the drug concentration is described by two convection-diffusion equations that are coupled by transference conditions at the contact boundary.

The main objective of this Chapter is the study of the drug concentrations in different scenarios and it is organized as follows. In Section 3.2 we establish the coupled model for the drug concentration. The stability analysis is presented in Section 3.3 using the energy method. The energy estimates are used in Section 3.4 to compute lower bounds for the absorbed drug mass. A semi-analytical approach to solve the drug coupled problem is presented in Section 3.5 which is a natural extension of the one presented in Chapter 2. We remark that due to it's complexity, we do not use such approach to solve the drug distribution. We introduce in Section 3.6 an explicit numerical method for the coupled convection-diffusion equations. The stability of the methods and its convergence are established under convergence assumptions on the time and space step sizes. Numerical results illustrating the drug distribution in different scenarios are included in Section 3.7.

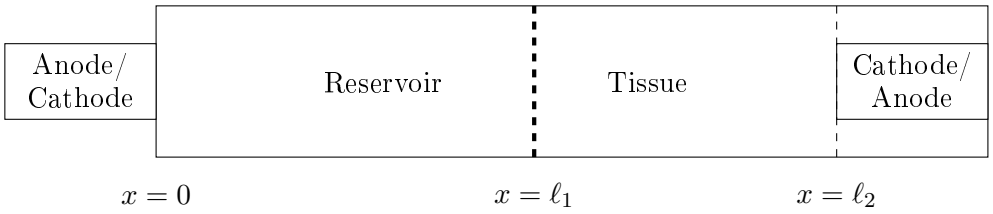

Figure 3.1: Considered coupled model.

3.2. The coupled drug distribution model

As illustrated in figure 3.1 we consider $[0, \ell_1]$ to be the reservoir and $[\ell_1, \ell_2]$ the target tissue, with $x = \ell_1$ the contact point, and denote $c_r(x,t)$ the drug concentration in $x \in [0, \ell_1]$ and $c_s(x,t)$ the drug concentration in $x \in [\ell_1, \ell_2]$ at time $t \geq 0$. We assume that the left-hand side of the reservoir is isolated and the drug molecules that reach the boundary $x = \ell_2$ are immediately removed. In the domains $(0, \ell_1)$ and (ℓ_1, ℓ_2) a diffusion process takes place enhanced by the electric field generated by the applied electric potential Φ at $x = 0$ and $x = \ell_2$, respectively, Φ_0 and Φ_1. We assume that the polymeric matrix of the reservoir and the target tissue have different electric conductivities σ_r and σ_s (S/m), respectively, as well as the drug has different diffusion coefficients in both media, D_r and D_s, respectively.

The electric field in each medium is given by $E_i = \sigma_i \nabla \Phi_i$, $i = r, s$ and, neglecting the electroosmosis transport, the drug mass flux in the reservoir J_r and in the target tissue J_s are given by

$$J_i = -D_i \nabla c_i - v_i c_i,\ i = r, s\,, \tag{3.1}$$

where c_i denotes the drug concentration in the medium $i = r, s$ and v_i is given by

$$v_i = \frac{z D_i F}{R T_i} \nabla \Phi_i,\ i = r, s\,, \tag{3.2}$$

where z denotes the valence of the drug molecules, F the Faraday constant, T_i the temperature in the medium $i = r, s$, and R the gas constant.

Solving the electric potential from the Laplace equation, with boundary conditions $\Phi_r(0) = \Phi_0$ and $\Phi_s(\ell_2) = \Phi_1$ and assuming at $x = \ell_1$ the continuity of the potentials and continuity of the electric field, the electric potentials Φ_i, $i = r, s$, are described by the systems

$$\begin{cases} \nabla \cdot (\sigma_r \nabla \Phi_r) = 0 \quad \text{in } (0, \ell_1) \\ \Phi_r(0) = \Phi_0 \end{cases} \tag{3.3}$$

and

$$\begin{cases} \nabla \cdot (\sigma_s \nabla \Phi_s) = 0 \quad \text{in } (\ell_1, \ell_2) \\ \Phi_s(\ell_2) = \Phi_1 \end{cases}, \tag{3.4}$$

coupled with the transition conditions

$$\begin{cases} \Phi_r(\ell_1) = \Phi_s(\ell_1) & \text{(continuity of the potential)} \\ \sigma_r \nabla \Phi_r(\ell_1) = \sigma_s \nabla \Phi_s(\ell_1) & \text{(continuity of the electric field)} \end{cases}. \tag{3.5}$$

We remark that the first condition of (3.5) can be seen on as the limit of the Robin type condition

$$J_r(\ell_1) = \alpha(\Phi_r(\ell_1) - \Phi_s(\ell_1)) \tag{3.6}$$

when $\alpha \to +\infty$.

The mass conservation law on each medium

$$\frac{\partial c_i}{\partial t} + \nabla \cdot J_i = 0,\ i = r, s, \tag{3.7}$$

together with (3.1) give us the convection-diffusion equations, for c_i, $i = r, s$,

$$\begin{cases} \dfrac{\partial c_r}{\partial t} = \nabla \cdot (D_r \nabla c_r) + \nabla \cdot (v_r c_r) \quad \text{in } (0, \ell_1) \times \mathbb{R}^+ \\ D_r \nabla c_r(0,t) + v_r c_r(0,t) = 0, \qquad t \in \mathbb{R}_0^+ \end{cases} \tag{3.8}$$

and

$$\begin{cases} \dfrac{\partial c_s}{\partial t} = \nabla \cdot (D_s \nabla c_s) + \nabla \cdot (v_s c_s) \quad \text{in } \in (\ell_1, \ell_2) \times \mathbb{R}^+ \\ c_s(\ell_2, t) = 0, \qquad t \in \mathbb{R}_0^+ \end{cases}. \tag{3.9}$$

System (3.8), (3.9) is complemented with the following interface conditions

$$\begin{cases} \gamma c_r(\ell_1, t) = c_s(\ell_1, t) & \text{(continuity of the concentration)} \\ J_r(\ell_1, t) = J_s(\ell_1, t) & \text{(continuity of the mass flux)} \end{cases}, \tag{3.10}$$

with $\gamma \in [0, 1]$, and initial condition

$$\begin{cases} c_r(x, 0) = c_{r,0}, \quad x \in (0, \ell_1) \\ c_s(x, 0) = 0, \qquad x \in (\ell_1, \ell_2) \end{cases}. \tag{3.11}$$

Conditions (3.11) mean that the reservoir is initially with a homogeneous drug distribution and that the target tissue is empty.

Solving the potential problems (3.3), (3.4) and (3.5) we obtain

$$\begin{cases} \Phi_r(x) = \dfrac{\Phi_1 - \Phi_0}{\ell_1 + \frac{\sigma_r}{\sigma_s}(\ell_2 - \ell_1)} x + \Phi_0, & x \in [0, \ell_1) \\ \Phi_s(x) = \dfrac{\sigma_r}{\sigma_s} \dfrac{\Phi_1 - \Phi_0}{\ell_1 + \frac{\sigma_r}{\sigma_s}(\ell_2 - \ell_1)} \big(x - \ell_2\big) + \Phi_1, & x \in [\ell_1, \ell_2] \end{cases} . \tag{3.12}$$

From (3.12) and (3.2) we deduce the convective velocities

$$\begin{cases} v_r = \dfrac{D_r z F}{R T_r} \dfrac{\Phi_1 - \Phi_0}{\ell_1 + \frac{\sigma_r}{\sigma_s}(\ell_2 - \ell_1)} \\ v_s = \dfrac{D_s z F}{R T_s} \dfrac{\sigma_r}{\sigma_s} \dfrac{\Phi_1 - \Phi_0}{\ell_1 + \frac{\sigma_r}{\sigma_s}(\ell_2 - \ell_1)} \end{cases} . \tag{3.13}$$

Finally the drug distribution in he reservoir r and in the target tissue s is described by (3.8)-(3.11) with the convective velocities given by (3.13).

3.3. Stability analysis

To study the stability of the coupled IBVP (3.8)-(3.11), (3.13) we introduce the space $V = \{w \in \mathbb{H}^1(0, \ell_2) : w(\ell_2) = 0\}$. Let D and v be defined by

$$D = \begin{cases} D_r, \, x \in (0, \ell_1) \\ \\ D_s, \, x \in (\ell_1, \ell_2) \end{cases} , \qquad v = \begin{cases} v_r, \, x \in (0, \ell_1) \\ \\ v_s, \, x \in (\ell_1, \ell_2) \end{cases} .$$

Then we replace the coupled IBVP for the drug evolution by the following initial value problem: find, for each $t \in \mathbb{R}^+$, $c(t) \in V$ such that $c'(t) \in \mathbb{L}^2(0, \ell_2)$ and

$$(c'(t), w) = -(D \nabla c(t), \nabla w) - (v c(t), \nabla w), t \in \mathbb{R}^+, \, \forall w \in V, \tag{3.14}$$

where $(.,.)$ denotes the usual inner product in $\mathbb{L}^2(0, \ell_2)$, and

$$c(0) = c_{r,0} \text{ in } [0, \ell_1], \quad c(0) = 0 \text{ in } (\ell_1, \ell_2]. \tag{3.15}$$

The drug distribution is then defined by

$$c_r(t) = c(t) \text{ in } [0, \ell_1], \quad c_s(t) = c(t) \text{ in } [\ell_1, \ell_2].$$

To study the stability of the weak problem (3.14)-(3.15) we recall that the following Friedrich-Poincaré inequality

$$\|w\|^2 \leq \frac{\ell_2^2}{2} \|\nabla w\|^2, \, w \in V, \tag{3.16}$$

holds. In the next results we establish energy estimates for $c(t)$:

Theorem 3. *If $c(t) \in V$ is a solution of (3.14), (3.15) then*

$$\|c(t)\|^2 \leq e^{\left(-\frac{2}{\ell_2^2}\min_{i=r,s} D_i + \max_{i=r,s}\frac{v_i^2}{D_i}\right)t}\|c(0)\|^2, t \in \mathbb{R}_0^+. \tag{3.17}$$

Proof. Taking in (3.14) $w = c(t)$ we have

$$\frac{d}{dt}\|c(t)\|^2 = -2\|\sqrt{D}\nabla c(t)\|^2 - 2(vc(t), \nabla c(t)). \tag{3.18}$$

As

$$2(vc(t), \nabla c(t)) \leq \sum_{i=r,s}\Big(v_i^2\frac{1}{2\varepsilon_i^2}\|c(t)\|_i^2 + 2\varepsilon_i^2\|\nabla c(t)\|_i^2\Big),$$

with $\varepsilon_i \neq 0$, where $\|.\|_i$, for $i = r, s$, denotes the $\mathbb{L}^2$ norm in the reservoir and in the target tissue, respectively, we deduce

$$\frac{d}{dt}\|c(t)\|^2 \leq \sum_{i=r,s}\Big(\big(-2D_i + 2\varepsilon_i^2\big)\|\nabla c(t)\|_i^2 + v_i^2\frac{1}{2\varepsilon_i^2}\|c(t)\|_i^2\Big).$$

If we fix now $\varepsilon_i^2 = \dfrac{1}{2}D_i$, then we establish

$$\frac{d}{dt}\|c(t)\|^2 \leq \sum_{i=r,s}\Big(-D_i\|\nabla c(t)\|_i^2 + \frac{v_i^2}{D_i}\|c(t)\|_i^2\Big),$$

that implies

$$\frac{d}{dt}\|c(t)\|^2 \leq -\min_{i=r,s} D_i\|\nabla c(t)\|^2 + \max_{i=r,s}\frac{v_i^2}{D_i}\|c(t)\|^2.$$

Applying the inequality (3.16) we obtain

$$\frac{d}{dt}\|c(t)\|^2 \leq \Big(-\frac{2}{\ell_2^2}\min_{i=r,s} D_i + \max_{i=r,s}\frac{v_i^2}{D_i}\Big)\|c(t)\|^2$$

that leads to (3.17). □

From Theorem 3 we conclude the stability of the IBVP (3.14), (3.15) for bounded time intervals and if $c(t)$, $\tilde{c}(t) \in V$ are solutions of this problem then $c(t) = \tilde{c}(t)$.

3.4. An estimate for the absorbed mass

The upper bound (3.17) can be used to study the qualitative behavior of the drug mass inside of the coupled system and the absorbed drug. Let

$$M(t) = \int_0^{\ell_2} c(x,t)\,dx, t \in \mathbb{R}_0^+,$$

be the drug mass in the coupled system. As

$$M(t) \leq \sqrt{\ell_2}\|c(t)\|,$$

from Theorem 3 we obtain an upper bound for such mass.

Corollary 1. *Under the assumptions of Theorem 3, we have*

$$M(t) \leq \sqrt{\ell_2} e^{\frac{1}{2}(-\frac{2}{\ell_2^2}\min_{i=r,s} D_i + \max_{i=r,s}\frac{v_i^2}{D_i})t}\|c(0)\|,\ t \in \mathbb{R}_0^+. \tag{3.19}$$

Moreover, if

$$\frac{\max_{i=r,s}\frac{v_i^2}{D_i}}{D_i} < \frac{2}{\ell_2^2}, i = r, s, \tag{3.20}$$

then

$$\lim_{t\to\infty} M(t) = 0 \ \ \textit{exponentially.} \tag{3.21}$$

■

Let $M_{abs}(t)$ be the absorbed mass. We have

$$M_{abs}(t) = M(0) - M(t), t \in \mathbb{R}_0^+.$$

and consequently

$$M_{abs}(t) \geq M(0) - \sqrt{\ell_2} e^{\frac{1}{2}(-\frac{2}{\ell_2^2}\min_{i=r,s} D_i + \max_{i=r,s}\frac{v_i^2}{D_i})t}\|c(0)\|, t \in \mathbb{R}_0^+. \tag{3.22}$$

We remark that condition (3.20) can be a reasonable assumption at least for thin reservoirs where ℓ_1 is small.

To obtain a second estimate for $M(t)$, we need to improve the estimate (3.17). From (3.18) we deduce

$$\frac{d}{dt}\|c(t)\|^2 \leq -2\min_{i=r,s} D_i\|\nabla c(t)\|^2 + 2\ell_2 \max_{i=r,s}|v_i|\|c(t)\|\|\nabla c(t)\|,$$

that leads to

$$\frac{d}{dt}\|c(t)\|^2 \leq \Big(-2\min_{i=r,s} D_i + \sqrt{2}\ell_2 \max_{i=r,s}|v_i|\Big)\|\nabla c(t)\|^2.$$

Assuming that

$$\frac{|v_i|}{D_i} < \frac{2\sqrt{2}}{\ell_2},\ i = r, s, \tag{3.23}$$

we obtain

$$\frac{d}{dt}\|c(t)\|^2 \leq \Big(-2\min_{i=r,s} D_i + \sqrt{2}\ell_2 \max_{i=r,s}|v_i|\Big)\frac{2}{\ell_2^2}\|c(t)\|^2,$$

and finally

$$\|c(t)\|^2 \leq e^{\frac{2}{\ell_2^2}\left(-2\min_{i=r,s} D_i + \sqrt{2}\ell_2 \max_{i=r,s}|v_i|\right)t}\|c(0)\|^2, t \in \mathbb{R}_0^+. \tag{3.24}$$

From the previous considerations we conclude that under the condition (3.23), we have

$$M(t) \leq \sqrt{\ell_2} e^{\frac{1}{\ell_2^2}\left(-2\min_{i=r,s} D_i + \sqrt{2}\ell_2 \max_{i=r,s}|v_i|\right)t}\|c(0)\|, t \in \mathbb{R}_0^+, \tag{3.25}$$

and

$$M_{abs}(t) \geq M(0) - \sqrt{\ell_2} e^{\frac{1}{\ell_2^2}\left(-2\min_{i=r,s} D_i + \sqrt{2}\ell_2 \max_{i=r,s}|v_i|\right)t} \|c(0)\|, t \in \mathbb{R}_0^+. \quad (3.26)$$

The condition (3.23) is less restrictive than the condition (3.20) and the upper bound of (3.19) for the drug mass in the reservoir-target tissue is grater than the upper bound in (3.25). To conclude this Section we finally observe that the estimates (3.22) and (3.26) allow the evaluation of lower bounds for the absorbed mass $M_{abs}(t)$ provided that such lower bounds are positive.

In figure 3.2 we plot the absorbed mass computed numerically using the numerical method that will be studied in Section 3.6 and the lower bounds (3.22) and (3.26) for $\ell_1 = 10^{-3}$, $\ell_2 = 1.2 \times 10^{-3}$, $T_r = T_s = 310.15$, $\sigma_r = 1.5 \times 10^{-5}$, $\sigma_s = 10^{-7}$, $c_{r,0} = 1$, $D_r = 0.65 \times 10^{-10}$, $D_s = 1 \times 10^{-10}$, $\Phi_0 = -0.0001$, $\Phi_1 = 0.0001$ and $z = -1$ in a 6 hour iontophoresis procedure.

We observe that, from lower bound (3.22), after $6h$ the absorbed mass is greater that $0.8mg$ and after $4h$ it is already at least $0.6mg$, while from (3.26) we conclude that after $6h$ it is greater than $0.5mg$, being the absorbed mass approximately $0.9mg$.

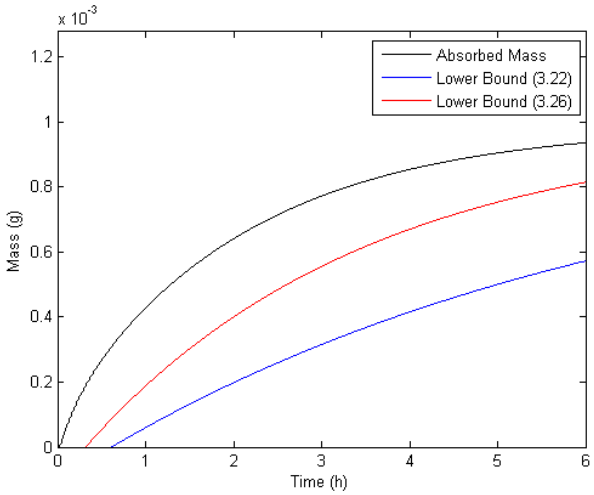

Figure 3.2: Absorbed mass at $x = \ell_2$ with the obtained lower bounds.

3.5. A semi-analytical Fourier method

In what follows we use the method of separation of variables to construct a solution for the coupled IBVP (3.8)-(3.11), (3.13). We remark that in [18] the same methodology was used for a coupled problem.

Assuming that $c_i(x,t) = M_i(x)N_i(t)$, for $i = r, s$, we obtain

$$M_i'' + \frac{v_i}{D_i} M_i' = \lambda_i M_i,\ N_i' = D_i \lambda_i N_i,\quad i = r, s\,. \tag{3.27}$$

Considering the new variables $\tilde{x} = \dfrac{x - \ell_1}{\ell_1}$ and $\tilde{M}_i(x) = e^{-\frac{v_i}{2D_i}x} M_i(x)$, for $i = r, s$, we can write the following spatial eigenvalue problems

$$\tilde{M}_r'' = \tilde{\lambda}_r \tilde{M}_r,\ \tilde{x} \in (-1, 0),\quad \tilde{M}_s'' = \tilde{\lambda}_s \tilde{M}_s,\ \tilde{x} \in (0, \tilde{\ell}) \tag{3.28}$$

with $\tilde{\lambda}_i = \frac{v_i^2}{4D_i} + \lambda_i$, for $i = r, s$, that are coupled with the following conditions

$$\begin{cases} D_r \tilde{M}_r'(-1) + \frac{3v_r}{2} \tilde{M}_r(-1) = 0 \\ \gamma \tilde{M}_r(0) = \tilde{M}_s \\ D_r \tilde{M}_r'(0) + \frac{3v_r}{2} \tilde{M}_r(0) = D_s \tilde{M}_s'(0) + \frac{3v_s}{2} \tilde{M}_s(0) \\ \tilde{M}_s(\tilde{\ell}) = 0 \end{cases}. \tag{3.29}$$

To obtain the desired Fourier series we need to solve (3.28) and (3.29). Let us suppose that $\tilde{\lambda}_i < 0$, otherwise we obtain an exponential representation of $\tilde{M}_i$, $i = r, s$. Replacing $\tilde{\lambda}_i$ by $-\tilde{\lambda}_i^2$, $i = r, s$, in (3.28) we obtain the eigenfunctions

$$\tilde{M}_i(\tilde{x}) = a_i \cos(\tilde{\lambda}_i \tilde{x}) + b_i \sin(\tilde{\lambda}_i \tilde{x}),\ i = r, s\,. \tag{3.30}$$

From conditions (3.29) we can write the linear system for a_r, b_r, a_s and b_s

$$\begin{bmatrix} D_r k_r \sin(\tilde{\lambda}_r) + \frac{3v_r}{2}\cos(\tilde{\lambda}_r) & D_r\tilde{\lambda}_r \cos(\tilde{\lambda}_r) + \frac{3v_r}{2}\sin(\tilde{\lambda}_r) & 0 & 0 \\ \gamma & 0 & -1 & 0 \\ \frac{3v_r}{2} & -D_r\tilde{\lambda}_r & -\frac{3v_s}{2} & D_s\tilde{\lambda}_s \\ 0 & 0 & \cos(\tilde{\lambda}_s\tilde{\ell}) & \sin(\tilde{\lambda}_s\tilde{\ell}) \end{bmatrix} \begin{bmatrix} a_r \\ b_r \\ a_s \\ b_s \end{bmatrix} = \begin{bmatrix} 0 \\ 0 \\ 0 \\ 0 \end{bmatrix} \tag{3.31}$$

System (3.31) admits the following solution

$$\begin{cases} a_s = \gamma a_r \\ b_r = \frac{\frac{3v_r}{2}(1-\gamma) + D_s\tilde{\lambda}_s \mathrm{cotg}(\tilde{\lambda}_s\tilde{\ell})}{D_r\tilde{\lambda}_r} a_r \\ b_s = -\gamma \mathrm{cotg}(\tilde{\lambda}_s\tilde{\ell}) a_r \end{cases} \tag{3.32}$$

for $a_s \in \mathbb{R}$ if and only if the matrix of this system is singular, that is,

$$\left(D_r\tilde{\lambda}_r \cos(\tilde{\lambda}_r) + \frac{3v_r}{2}\sin(\tilde{\lambda}_r)\right)\left(\gamma D_s\tilde{\lambda}_s \cos(\tilde{\lambda}_s\tilde{\ell}) + \sin(\tilde{\lambda}_s\tilde{\ell})\frac{3(\gamma v_s - v_r)}{2}\right) + \left(D_r k_r \sin(\tilde{\lambda}_r) + \frac{3v_r}{2}\cos(\tilde{\lambda}_r)\right)(-D_r\tilde{\lambda}_r \sin(\tilde{\lambda}_s\tilde{\ell})) = 0 \tag{3.33}$$

As we have

$$N_i(t) = e^{D_i\lambda_i t}N_i(0), \quad i = r, s\,,$$

we obtain

$$c_i(x,t) = e^{D_i\lambda_i t}N_i(0)M_i(x), \quad i = r, s\,.$$

The first interface condition at $x = \ell_1$ holds if and only if

$$\gamma e^{D_r\lambda_r t}N_r(0)M_r(0) = e^{D_s\lambda_s t}N_s(0)M_s(0)\,.$$

As $\gamma\tilde{M}_r(0) = \tilde{M}_s(0)$ we conclude that

$$\tilde{M}_s(0)\left[e^{D_r\lambda_r t}N_r(0) - e^{D_s\lambda_s t}N_s(0)\right] = 0$$

which implies $\tilde{M}_s(0) = 0$ or $e^{D_r\lambda_r t}N_r(0) = e^{D_s\lambda_s t}N_s(0)$. Since $\tilde{M}_s(0) = 0$ leads to the null solutions $\tilde{M}_i$, $i = r, s$, we set

$$e^{D_r\lambda_r t}N_r(0) = e^{D_s\lambda_s t}N_s(0)$$

for any initial condition. This implies in particular that

$$D_r\lambda_r = D_s\lambda_s\,. \tag{3.34}$$

Equations (3.33) and (3.34) should lead to a set of eigenvalues λ_i, $i = r, s$, and then using (3.32), the corresponding eigenfunctions $\tilde{M}_i$, $i = r, s$ are obtained. Finally using N_i, $i = r, s$, we obtain c_i, $i = r, s$.

The procedure described before, requires the use of a numerical method to solve equations (3.33) and (3.34) because we are not able to obtain explicit expressions for λ_r and λ_s. Then, using the corresponding values, we get the corresponding eigenfunctions.

The complexity of the presented Fourier method is a motivation for the next section, where we present a numerical method to solve the IBVP (3.8) - (3.10).

3.6. A discrete approach

3.6.1. An explicit Euler method

Let $T > 0$ be fixed and $Q = [0, \ell_2] \times [0, T]$. Given $N \geq 4$ and $M \geq 1$ integers, let $h = \ell_2/N$ and $\Delta t = T/M$, we define the non-uniform mesh $Q_h^{\Delta t}$ on Q by

$$Q_h^{\Delta t} = \{(x_i, t_m) : x_1 = 0;\, x_N = \ell_2;\, x_{i+1} - x_i = h_i, 0 \leq i \leq N;\, t_m = m\Delta t, 0 \leq m \leq M\}$$

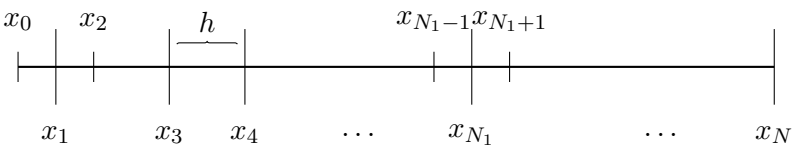

Figure 3.3: Spatial grid.

where x_0 is an auxiliary point, x_{N_1} is the transition point and h_i is given by

$$x_{i+1} - x_i = h_i = \begin{cases} \frac{h}{2}, & i \in \{0, 1, N_1, N_1 + 1\} \\ h, & i \in \{2, ..., N_1 - 1, N_1 + 2, ..., N\} \end{cases} . \tag{3.35}$$

The spatial grid is illustrated in figure 3.3.

By D_x^+, D_x^- we denote the usual forward and backward finite difference operators on space respectively. The first and second order centered finite difference operators are denoted by D_x^c and D_x^2, respectively. Finally we introduce the notation for the backward finite difference operator in time D_t^-. By $U_{i,l}^m$ we represent the approximation of the solution for $c_i(x_l, t_m)$, for $i = r, s$ defined by

$$\begin{cases} D_t^- U_{r,i}^m = D_r D_x^2 U_{r,i}^m + D_x^c v_r U_{r,i}^m , & i \in \{1, ..., N_1 - 1\} \\ U_{r,i}^0 = c_{r,0} , & i \in \{1, ..., N_1 - 1\} \\ D_r D_x^c U_{r,1}^m + \frac{v_r (U_{r,0}^m + 2U_{r,1}^m + U_{r,2}^m)}{4} = 0 , & m \geq 0 , \end{cases} \tag{3.36}$$

$$\begin{cases} D_t^- U_{s,i}^m = D_r D_x^2 U_{s,i}^m + D_x^c v_s U_{s,i}^m , & i \in \{N_1 + 1, ..., N - 1\} \\ U_{s,i}^0 = 0 , & i \in \{N_1 + 1, ..., N - 1\} \\ U_{s,N}^m = 0 , & m \geq 0 , \end{cases} \tag{3.37}$$

with the transition conditions

$$\begin{cases} D_r D_x^- U_{r,N_1}^m + v_r \frac{U_{r,N_1-1}^m + U_{r,N_1}^m}{2} = D_s D_x^+ U_{s,N_1}^m + v_s \frac{U_{s,N_1}^m + U_{s,N_1+1}^m}{2}, & m \geq 0 \\ \gamma U_{r,N_1}^m = U_{s,N_1}^m , & m \geq 0 . \end{cases} \tag{3.38}$$

To obtain a matrix representation of the finite differene method, we start by solving the last equation of (3.36) for $U_{r,0}^m$. We obtain

$$U_{r,0}^m = \frac{2v_r h}{4D_r - v_r h} U_{r,1}^m + \frac{4D_r + v_r h}{4D_r - v_r h} U_{r,2}^m$$

and considering now this expression in the first equation of (3.36) for $i = 1$ we deduce

$$U_{r,1}^m = \left(1 - 8D_r \frac{\Delta t}{h^2} + 2D_r \frac{\Delta t}{h}\right) U_{r,1}^{m-1} + 2\frac{\Delta t}{h^2} (4D_r + v_r h) U_{r,2}^{m-1} .$$

Taking $i = 2$ in the first equation of (3.36) we get

$$\begin{aligned} U_{r,2}^m &= \frac{2}{3}\frac{\Delta t}{h^2}\left(4D_r - v_r h\right) U_{r,1}^{m-1} + \left(1 - 4\frac{\Delta t}{h^2}D_r\right) U_{r,2}^{m-1} \\ &+ \frac{2}{3}\frac{\Delta t}{h^2}\left(D_r + v_r h\right) U_{r,3}^{m-1}. \end{aligned}$$

For $i \in \{3, ..., N_1 - 2\}$ we have

$$\begin{aligned} U_{r,i}^m &= \frac{\Delta t}{h^2}\left(D_r - v_r h)\right) U_{r,i-1}^{m-1} + \left(1 - 2\frac{\Delta t}{h^2}D_r\right) U_{r,i}^{m-1} \\ &+ \frac{\Delta t}{h^2}\left(D_r + v_r h)\right) U_{r,i+1}^{m-1}. \end{aligned}$$

From the system (3.38) we obtain

$$\begin{aligned} U_{r,N_1}^m &= \left(\frac{4D_r - v_r h}{4(\gamma D_s + D_r) + (v_r - \gamma v_s)h}\right) U_{r,N_1-1}^m \\ &- \left(\frac{4D_s + v_s h}{4(\gamma D_s + D_r) + (v_r - \gamma v_s)h}\right) U_{s,N_1+1}^m. \end{aligned}$$

Considering this result in the first equation of (3.36) for $i = N_1 - 1$ and in the first equation of (3.37) for $i = N_1 + 1$ we establish

$$\begin{aligned} U_{r,N_1-1}^m &= \frac{2}{3}\frac{\Delta t}{h^2}\left(2D_r - v_r h\right) U_{N_1-2}^{m-1} \\ &+ \left(1 - 4\frac{\Delta t}{h^2}D_r + \frac{2}{3}\frac{\Delta t}{h^2}\frac{(2D_r + v_r h)(4D_s - v_s h)}{4(D_r + \gamma D_s) + h(v_r - \gamma v_s)}\right) U_{r,N_1-1}^{m-1} \\ &+ \frac{2}{3}\frac{\Delta t}{h^2}\left(\frac{(2D_r + v_r h)(4D_s + v_s h)}{4(D_r + \gamma D_s) + h(v_r - \gamma v_s)}\right) U_{s,N_1+1}^{m-1} \end{aligned}$$

and

$$\begin{aligned} U_{s,N_1+1}^m &= \frac{2}{3}\frac{\Delta t}{h^2}\left(\frac{(2D_s - v_s h)(4D_r - v_r h)}{4(D_r + \gamma D_s) + h(v_r - \gamma v_s)}\right) U_{r,N_1-1}^{m-1} \\ &+ \left(1 + 4\frac{\Delta t}{h^2}D_s + \frac{2}{3}\frac{\Delta t}{h^2}\frac{(2D_s - v_s h)(4D_s + v_s h)}{4(D_r + \gamma D_s) + h(v_r - \gamma v_s)}\right) U_{s,N_1+1}^{m-1} \\ &+ \frac{2}{3}\frac{\Delta t}{h^2}\left(2D_s + v_s h\right) U_{s,N_1+2}^{m-1}. \end{aligned}$$

Finally when $i \in \{N_1 + 2, ..., N - 1\}$ we have

$$\begin{aligned} U_{s,i}^m &= \frac{\Delta t}{h^2}\left(D_s - v_s h\right) U_{s,i-1}^{m-1} + \left(1 - 2\frac{\Delta t}{h^2}D_s\right) U_{s,i}^{m-1} \\ &+ \frac{\Delta t}{h^2}\left(D_s + v_s h\right) U_{s,i+1}^{m-1}, \end{aligned}$$

respectively.

The previous system can be rewritten in the following equivalent form

$$U^{m+1} = A_{h,\Delta t} U^m,\ m = 1, \ldots, M, \tag{3.39}$$

where $U_i^m = U_{r,i}^m$, for $i \in \{1, \ldots, N_1 - 1\}$, $U_i^m = U_{s,i}^m$, for $i \in \{N_1 + 1, \ldots, N\}$ and U^0 is known.

3.6.2. Stability

From (3.39) we obtain

$$\left\|U^{m+1}\right\|_\infty \leq \|A_{h,\Delta t}\|_\infty^m \left\|U^0\right\|_\infty .$$

Then

$$\|U^m\|_\infty \leq \left\|U^0\right\|_\infty \tag{3.40}$$

provided that $\|A_{h,\Delta t}\|_\infty \leq 1$. Inequality (3.40) means that that the operator $A_{h,\Delta t}$ is stable.

In what follows we take $\gamma = 1$. Recalling the observations from figures 2.2 and 2.3, and taking into account that v_i is given by (3.13), we have $v_i < 0$, for $i = r, s$. We shall impose a set of conditions on the time and space step sizes that lead to $\|A_{h,\Delta t}\|_\infty \leq 1$.

Let A_1 be the first line of $A_{h,\Delta t}$. We have

$$\|A_1\|_1 = 2\frac{\Delta t}{h^2}|4D_r + v_r h| + |1 - 2\frac{\Delta t}{h^2}(D_r - v_r h)| .$$

If

$$h < \frac{4D_r}{-v_r} \tag{3.41}$$

and

$$2\frac{\Delta t}{h^2}(4D_r - v_r h) < 1 \tag{3.42}$$

we get $\|A_1\|_1 = 1$.

For the second line of $A_{h,\Delta t}$ we deduce

$$\|A_2\|_1 = 2\frac{\Delta t}{h^2}(4D_r - v_r h) + \left|1 - 4\frac{\Delta t}{h^2}D_r\right| + \frac{2}{3}\frac{\Delta t}{h^2}|2D_r + v_r h| .$$

If

$$h < \frac{2D_r}{-v_r} \tag{3.43}$$

and

$$\frac{\Delta t}{h^2} < \frac{1}{4D_r} \tag{3.44}$$

we can conclude $\|A_2\|_1 = 1$. We remark that (3.43) implies (3.41), while (3.42) and (3.43) implies (3.44).

For the lines A_i, $i \in \{3, \ldots, N_1 - 1\}$ of matrix $A_{h,\Delta t}$ we have

$$\|A_i\|_1 = 2\frac{\Delta t}{h^2}(D_r - h\frac{v_r}{2}) + \left|1 - 2\frac{\Delta t}{h^2}D_r\right| + \frac{\Delta t}{h^2}|D_r + v_r h|$$

and conditions (3.44), (3.43) allow us to write $\|A_i\|_1 = 1$.

For the line A_{N_1-1} we deduce

$$\begin{aligned}\|A_{N_1-1}\|_1 &= \frac{2}{3}\frac{\Delta t}{h^2}(2D_r - v_r h)\\ &+ \left|1 - 4\frac{\Delta t}{h^2}D_r + \frac{2}{3}\frac{\Delta t}{h^2}\frac{(2D_r + v_r h)(4D_r - v_r h)}{4(D_r + D_s) + h(v_r - v_s)}\right|\\ &+ \frac{2}{3}\frac{\Delta t}{h^2}\left|\frac{(2D_r + v_r h)(4D_s + v_s h)}{4(D_r + D_s) + h(v_r - v_s)}\right|.\end{aligned}$$

If $v_s - v_r > 0$ then for $h < \frac{4(D_r+D_s)}{v_s - v_r}$, $h < 2\frac{D_r}{-v_r}$, $\frac{\Delta t}{h^2} < \frac{1}{4D_r}$ and $h < \frac{4D_s}{-v_s}$ we obtain

$$\begin{aligned}\|A_{N_1-1}\|_1 &= \frac{2}{3}\frac{\Delta t}{h^2}(2D_r - v_r h) + 1 - 4\frac{\Delta t}{h^2}D_r + \frac{2}{3}\frac{\Delta t}{h^2}(2D_r + v_r h)\frac{4(D_r + D_s) - h(v_r - v_s)}{4(D_r + D_s) + h(v_r - v_s)}\\ &\leq 1 - 4\frac{\Delta t}{h^2}D_r + \frac{8}{3}\frac{\Delta t}{h^2}D_r\\ &\leq 1.\end{aligned}$$

The line A_{N_1} satisfies

$$\begin{aligned}\|A_{N_1}\|_1 &= \frac{2}{3}\frac{\Delta t}{h^2}\frac{(2D_s - v_s h)(4D_r - v_r h)}{4(D_r + D_s) + h(v_r - v_s)}\\ &+ \left|1 - 4\frac{\Delta t}{h^2}D_s + \frac{2}{3}\frac{\Delta t}{h^2}\frac{(2D_s - v_s h)(4D_s + v_s h)}{4(D_r + D_s) + h(v_r - v_s)}\right|\\ &+ \left|\frac{2}{3}\frac{\Delta t}{h^2}(2D_s + v_s h)\right|.\end{aligned}$$

Since $v_i < 0$ for $i = r, s$, $h < \frac{2D_s}{-v_s}$, $h < \frac{4(D_r+D_s)}{v_s - v_r}$, $\frac{\Delta t}{h^2} < \frac{1}{4D_s}$, we obtain $\|A_{N_1}\|_1 \leq 1$.

For $i \in \{N_1 + 1, \ldots, N-1\}$, the lines A_{i-1} satisfy

$$\|A_{i-1}\|_1 = \frac{\Delta t}{h^2}|(D_s - v_s h)| + \left|1 - 2\frac{\Delta t}{h^2}D_s\right| + \frac{\Delta t}{h^2}(D_s + v_s h).$$

Assuming $h < \frac{D_s}{-v_s}$, $\frac{\Delta t}{h^2} < \frac{1}{2D_s}$ we get $\|A_{i-1}\|_1 = 1$, for $i \in \{N_1 + 1, \ldots, N-1\}$.

The following proposition summarizes the previous conclusions:

Proposition 1. *If $\gamma = 1$, $v_s - v_r > 0$, where v_r and v_s are defined by (3.13) and*

$$h < 2\min_{i=r,s}\frac{D_i}{-v_i}, \quad (3.43) \qquad \frac{\Delta t}{h^2} < \min_{i=1,2}\frac{1}{4D_i}, \quad (3.44) \qquad h \leq \frac{4(D_r + D_s)}{v_r - v_s}, \quad (3.45)$$

then the finite difference scheme (3.39) is stable. If $v_s - v_r < 0$ then the scheme is stable under the assumptions (3.43) and (3.44).

In figure 3.4 we plot the drug concentration obtained with parameters which violate condition (3.44). We used $\ell_1 = 10^{-3}$, $\ell_2 = 1.2 \times 10^{-3}$, $T_r = T_s = 37^o C$, $D_r = 10^{-11}$, $D_s = 10^{-12}$, $\sigma_r = 1.5 \times 10^{-5}$, $\sigma_s = 10^{-7}$, $c(x, 0) = 1, x \in (0, \ell_1)$, $c(x, 0) = 0, x \in (\ell_1, \ell_2)$, $z = -1$, $\Phi_0 = -0.5$, and $\Phi_1 = 1$. The discretization parameters where $N = 65$, $M = 10000$ which leads to $h \approx 1.85 \times 10^{-5}$ and $\Delta t = 2.16$. We remark the instability that is observed near the point $x = \ell_2$.

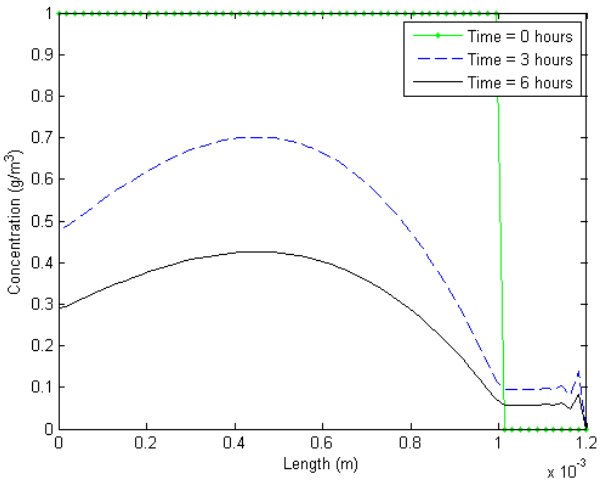

Figure 3.4: Representation of the instability.

3.6.3. Convergence

The convergence analysis is based on the stability Proposition 1 and in the consistency of the method (3.39). By $T_{h,\Delta t}$ we represent the truncation error induced by (3.39). Let $e^l_{h,\Delta t}(x_i,t_m)$, $l=r,s$ be the error of the numerical approximation U^m_i, for $i=1,\ldots,N_1-1,N_1,N_1+1,\ldots,N$. The errors $e_{h,\Delta t}$ and $T_{h,\Delta t}$ satisfy

- $$D_r D^c_x e^r_{h,\Delta t}(x_1,t_m)+v_r\frac{e^r_{h,\Delta t}(x_0,t_m)+2e^r_{h,\Delta t}(x_1,t_m)+e^r_{h,\Delta t}(x_2,t_m)}{4} = T_{h,\Delta t}(x_1,t_m)\,,$$

- $$D^-_t e^r_{h,\Delta t}(x_i,t_m)=D_r D^2_x e^r_{h,\Delta t}(x_i,t_m)+D^c_x(v_r e^r_{h,\Delta t}(x_i,t_m)) + T_{h,\Delta t}(x_i,t_m),\ i=2,3,\ldots,N_1-1\,,$$

- $$\gamma e^r_{h,\Delta t}(x_{N_1},t_m)=e^s_{h,\Delta t}(x_{N_1},t_m)\,,$$

- $$D_r D^-_x e^r_{h,\Delta t}(x_{N_1-1},t_m)+v_r\frac{e^r_{h,\Delta t}(x_{N_1},t_m)+e^r_{h,\Delta t}(x_{N_1},t_m)}{2} = D_s D^+_x e^s_{h,\Delta t}(x_{N_1},t_m)+v_s\frac{e^s_{h,\Delta t}(x_{N_1},t_m)+e^s_{h,\Delta t}(x_{N_1+1},t_m)}{2} + T_{h,\Delta t}(x_{N_1-1},t_m)\,,$$

- $$D^-_t e^s_{h,\Delta t}(x_i,t_m)=D_s D^2_x e^s_{h,\Delta t}(x_i,t_m)+D^c_x(v_s e^s_{h,\Delta t}(x_i,t_m)) + T_{h,\Delta t}(x_i,t_m),\ i=N_1+1,\ldots,N-1\,.$$

It is easy to show that

$$D_t^- c_l(x_i,t_m) = \frac{\partial c_l}{\partial t}(x_i,t_m) + \mathcal{O}(\Delta t)\,, \tag{3.46}$$

$$D_x^+ c_l(x_i,t_m) = \frac{\partial c_l}{\partial x}(x_i,t_m) + \mathcal{O}(h_{i+1})\,, \tag{3.47}$$

$$D_x^- c_l(x_i,t_m) = \frac{\partial c_l}{\partial x}(x_i,t_m) + \mathcal{O}(h_i)\,, \tag{3.48}$$

$$\begin{aligned} D_x^c c_l(x_i,t_m) &= \frac{\partial c_l}{\partial x}(x_i,t_m) + \mathcal{O}\left(\frac{h_{i+1}-h_i}{2} + \frac{h_{i+1}^3+h_i^3}{6(h_{i+1}+h_i)}\right) \\ &= \frac{\partial c_l}{\partial x}(x_i,t_m) + \begin{cases} \mathcal{O}\left(h^2\right), & h_i = h_{i+1} \\ \mathcal{O}\left(h\right), & h_i \neq h_{i+1} \end{cases}, \end{aligned} \tag{3.49}$$

$$\begin{aligned} D_x^2 c_l(x_i,t_m) &= \frac{\partial^2 c_l}{\partial x^2}(x_i,t_m) + \mathcal{O}\left(\frac{h_{i+1}-h_i}{3} + \frac{h_i h_{i+1}^4 + h_{i+1} h_i^4}{12(h_i+h_{i+1})}\right) \\ &= \frac{\partial^2 c_l}{\partial x^2}(x_i,t_m) + \begin{cases} \mathcal{O}\left(h^2\right), & h_i = h_{i+1} \\ \mathcal{O}\left(h\right), & h_i \neq h_{i+1} \end{cases}, \end{aligned} \tag{3.50}$$

for $i \in \{1,\ldots,N_1-1\}$ if $l = r$ and $i \in \{N_1+1,\ldots,N-1\}$ if $l = s$, with $m \in \{1,\ldots,M\}$. From the previous considerations, it is easy to conclude

$$T_{h,\Delta t}(x_i,t_m) = \begin{cases} \mathcal{O}\left(h+\Delta t\right), & i \in \{2, N_1-1, N_1+1\},\ m \in \{1,\ldots,M\} \\ \mathcal{O}\left(h^2+\Delta t\right), & i \notin \{2, N_1-1, N_1+1\},\ m \in \{1,\ldots,M\} \end{cases} \tag{3.51}$$

which leads to $|T_{h,\Delta t}(x_i,t_m)| = \mathcal{O}(h+\Delta t)$, for $i = 1,2,\ldots,N-1$.

Let $e_{h,\Delta t}(t_m)$ be defined as U^m. Then it can be shown that

$$e_{h,\Delta t}(t_m) = A_{h,\Delta t}\, e_{h,\Delta t}(t_{m-1}) + \Delta t\, \tilde{T}_{h,\Delta t}(t_m)\,, \tag{3.52}$$

where $\tilde{T}_{h,\Delta t}(t_m)$ depends on $T_{h,\Delta t}(t_m)$ and satisfies $\left\|\tilde{T}_{h,\Delta t}(t_m)\right\|_\infty = \mathcal{O}\left(h+\Delta t\right)$. From (3.52) we obtain

$$\left\|e_{h,\Delta t}(t_m)\right\|_\infty \leq \left\|A_{h,\Delta t}\right\|_\infty \left\|e_{h,\Delta t}(t_{m-1})\right\|_\infty + \Delta t \left\|\tilde{T}_{h,\Delta t}(t_m)\right\|_\infty .$$

Under the assumptions of Proposition 1, we deduce

$$\left\|e_{h,\Delta t}(t_m)\right\|_\infty \leq \left\|e_{h,\Delta t}(t_{m-1})\right\|_\infty + \Delta t \left\|\tilde{T}_{h,\Delta t}(t_m)\right\|_\infty$$

and it follows that

$$\left\|e_{h,\Delta t}(t_m)\right\|_\infty \leq T \max_{1\leq j\leq M} \left\|\tilde{T}_{h,\Delta t}(t_j)\right\|_\infty \tag{3.53}$$

because $\left\|e_{h,\Delta t}(t_0)\right\|_\infty = 0$. Inequality (3.53) means that the proposed method is convergent.

In what follows we illustrate the convergence of the method under the assumptions stated in Proposition 1.

An illustration of the spatial order of convergence and associated error in norm $\|\cdot\|_\infty$ is given in comparison with a solution obtained with very small $h = 4.6 \times 10^{-6}$ and $\Delta t = 0.165$. In figures 3.5 we plot the reference solution and numerical approximations obtained with $\ell_1 = 10^{-3}$, $\ell_2 = 1.2 \times 10^{-3}$, $T_r = T_s = 37^oC$, $D_r = 10^{-11}$, $D_s = 10^{-12}$, $\sigma_r = 1.5 \times 10^{-5}$, $\sigma_s = 10^{-7}$, $c(x,0) = 1, x \in (0, \ell_1)$, $c(x,0) = 0, x \in (\ell_1, \ell_2)$, $z = -1$, $\Phi_0 = -0.05$, $\Phi_1 = 0.05$ and $T = 6$h. As it can be seen, an increase of the number of spatial points leads to a decrease of the associated error.

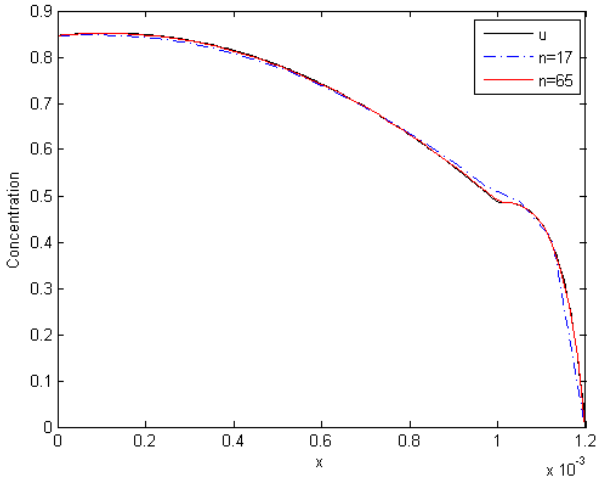

Figure 3.5: Error of the approximation.

In figure 3.6 we plot the errors $\|e_{h,\Delta t}(T)\|_\infty$.

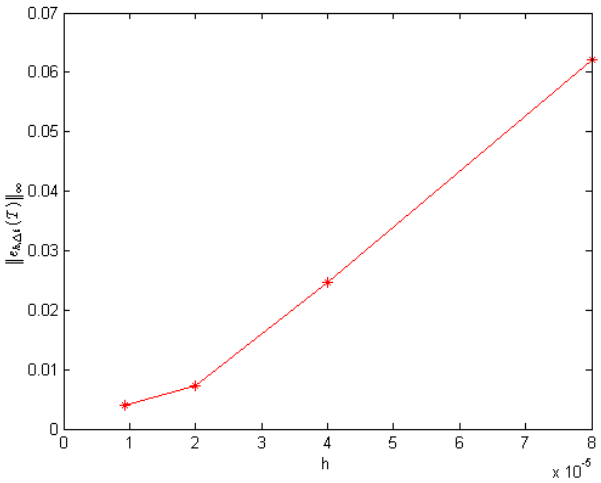

Figure 3.6: Spatial error.

3.7. Numerical Results

The objective of this Section is the illustration of the behavior of the drug concentration for the parameters previously used in the convergence experiments.

In figure 3.7 we plot the drug concentration when $v_i = 0$, $i = r, s$, this means that the transport phenomena occur only by diffusion. As time evolves, the value of the drug concentration decreases, mainly in the reservoir. To illustrate the effect of the electric field, we plot in figure 3.8 the numerical results obtained considering $\Phi_0 = -0.05$ and $\Phi_1 = 0.05$. From figures 3.7 and 3.8 we conclude that the drug release from the reservoir as well as the entrance in the target tissue and absorption in $x = \ell_2$ is enhanced by the applied potential. The drug concentrations obtained with $\Phi_0 = -0.5$, $\Phi_1 = 1$ are plotted in figure 3.9. From the figures 3.7 - 3.9 we can infer that an increase of the strength of the electric field is followed by a decrease of the drug concentrations.

The absorbed mass drug at $x = \ell_2$, $M(t)$, is presented in figure 3.10 for $v_r = v_s = 0$. The corresponding absorbed mass when an electric potential is applied, for $\Phi_0 = -0.05$, $\Phi_1 = 0.05$ and $\Phi_0 = -0.5$, $\Phi_1 = 1$ are plotted in figures 3.11 and 3.12. As before, we conclude that as the electric field increases, the drug delivery process increases as well, and consequently, the absorbed mass. The same conclusions are obtained from figures 3.13 - 3.15, where we plot the mass drug fluxes at $x = \ell_2$.

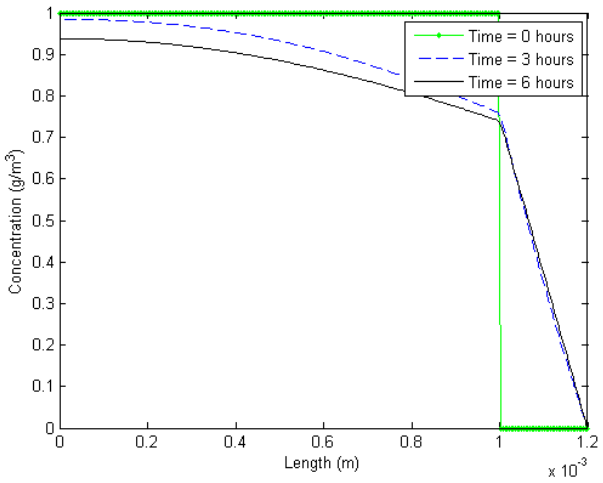

Figure 3.7: Drug concentration in the coupled system with diffusion only.

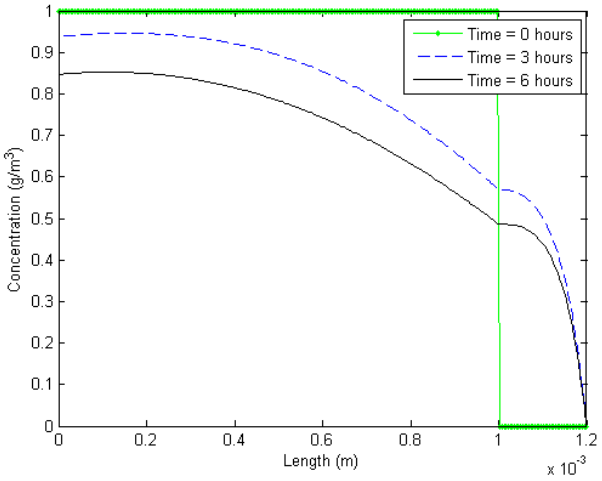

Figure 3.8: Drug concentration in the coupled system with $\Phi_0 = -0.05$, $\Phi_1 = 0.05$.

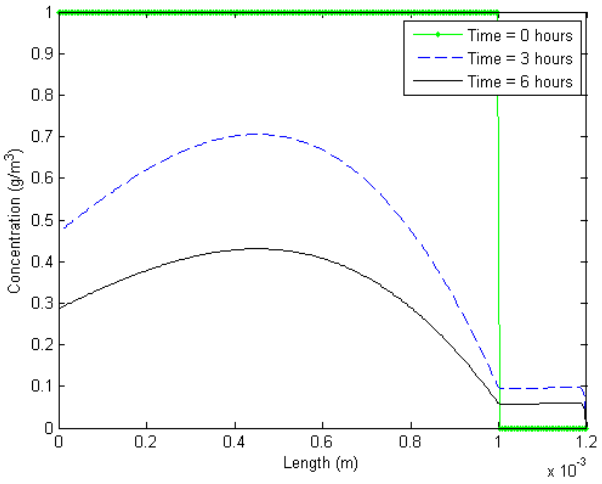

Figure 3.9: Drug concentration in the coupled system with $\Phi_0 = -0.5$, $\Phi_1 = 1$.

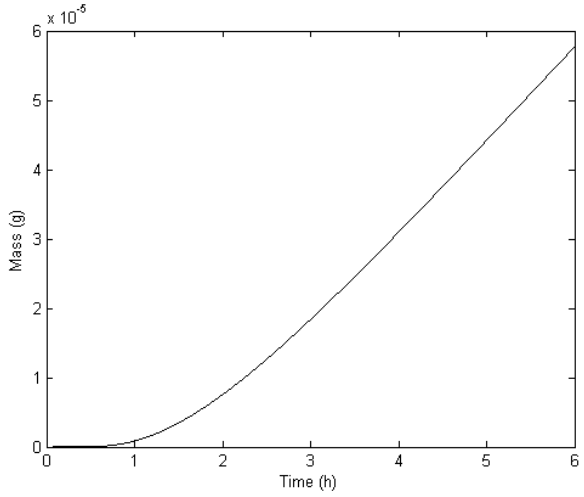

Figure 3.10: Absorbed mass at $x = \ell_2$ with diffusion only.

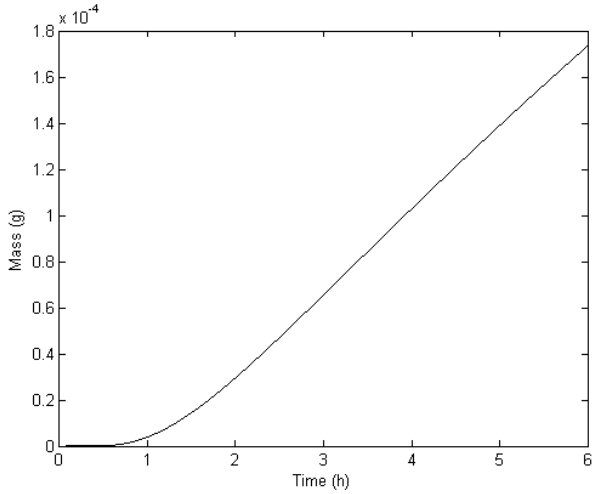

Figure 3.11: Absorbed mass at $x = \ell_2$ with $\Phi_0 = -0.05$, $\Phi_1 = 0.05$.

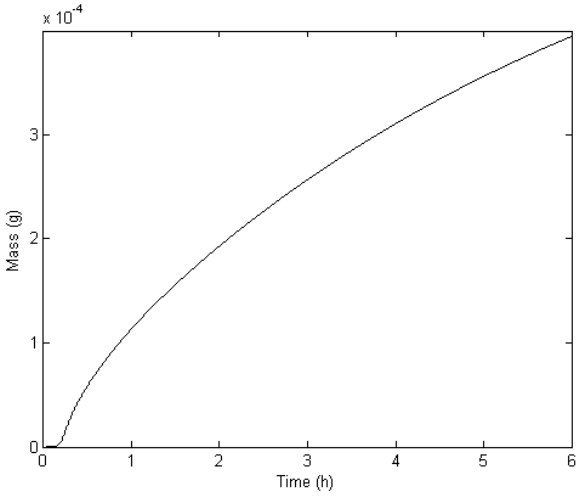

Figure 3.12: Absorbed mass at $x = \ell_2$ with $\Phi_0 = -0.5$, $\Phi_1 = 1$.

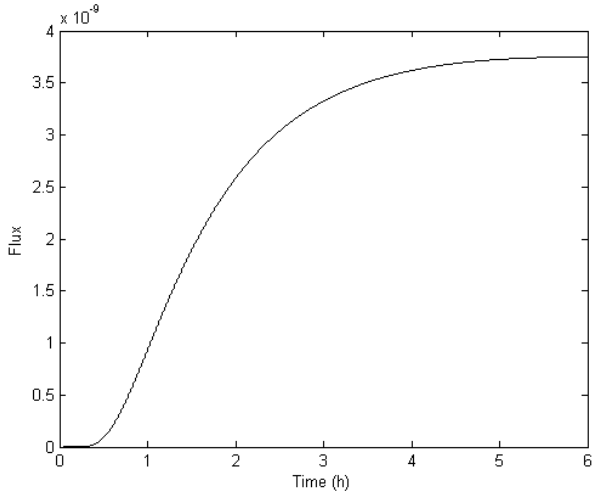

Figure 3.13: Drug flux at $x = \ell_2$ with diffusion only.

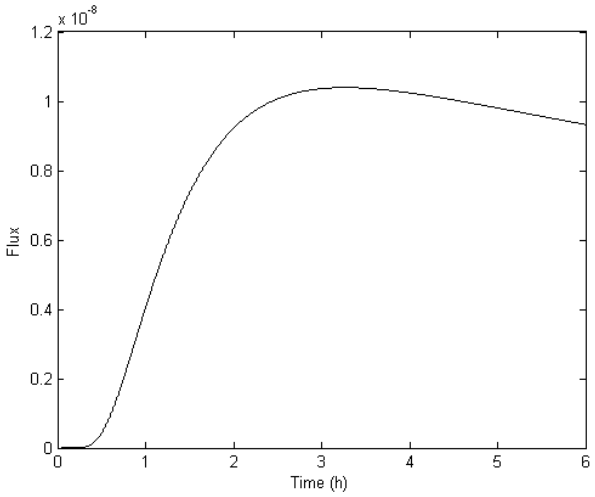

Figure 3.14: Drug flux at $x = \ell_2$ with $\Phi_0 = -0.05$, $\Phi_1 = 0.05$.

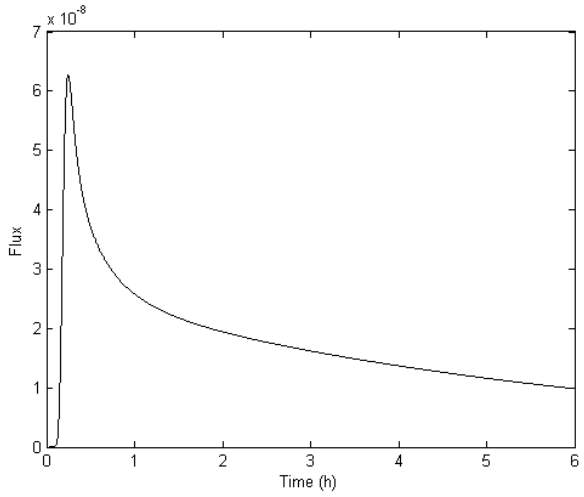

Figure 3.15: Drug flux at $x = \ell_2$ with $\Phi_0 = -0.5$, $\Phi_1 = 1$.

Chapter 4

Conclusions

In this work we studied the drug delivery of electric charged drugs from a polymeric reservoir and its entrance in a target tissue. To enhance the diffusion transport in the reservoir and in the target tissue, an applied potential is considered. This potential induces a convective mass flux that increases the drug release.

To simplify our study, in Chapter 2 we assume that the drug is in contact with the target tissue and that the drug release is described by a convection-diffusion equation where the convective velocity is given by the Nernst-Planck equation. In Chapter 3 we consider that the drug is contained in a reservoir which is in contact with the target tissue. In this case, the drug transport and its absorption in by the target tissue is described by two convection-diffusion equations that are coupled at the contact boundary. In both chapters we consider isotropic media which lead to 1D mathematical models, and the absorption of the drug in the target tissue was defined by a homogenous Drichlet boundary condition.

Two questions need to be object of study: the drug release of a polymeric reservoir when the drug absorption is described by a Robin boundary condition and when an anisotropic media is considered. This last assumption leads to 2D and 3D mathematical models.

The drug release was studied during a continuous period of application of the electric potential. In iontophoretic applications, the potential is applied during a certain time period which is followed by a rest period. This means that the boundary conditions defining the electric potentials are step functions. In the near future we intend to extend the obtained results to these more realistic situations.

Bibliography

[1] Ajay K Banga, Sagarika Bose, and Tapash K Ghosh. Iontophoresis and electroporation: comparisons and contrasts. *International journal of pharmaceutics*, 179(1):1–19, 1999.

[2] Sid Becker. Transport modeling of skin electroporation and the thermal behavior of the stratum corneum. *International Journal of Thermal Sciences*, 54:48–61, 2012.

[3] Sid Becker, Barbara Zorec, Damijan Miklavčič, and Nataša Pavšelj. Transdermal transport pathway creation: Electroporation pulse order. *Mathematical biosciences*, 257:60–68, 2014.

[4] James D Byrne, Mohammad NR Jajja, Adrian T OâĂŹNeill, Lissett R Bickford, Amanda W Keeler, Nabeel Hyder, Kyle Wagner, Allison Deal, Ryan E Little, Richard A Moffitt, et al. Local iontophoretic administration of cytotoxic therapies to solid tumors. *Science translational medicine*, 7(273):273ra14–273ra14, 2015.

[5] M Begona Delgado-Charro and Richard H Guy. Iontophoresis: applications in drug delivery and noninvasive monitoring. *Transdermal Drug Delivery Systems: Revised and Expanded*, page 199, 2002.

[6] Nitin Dixit, Vikas Bali, Sanjula Baboota, Alka Ahuja, and Javed Ali. Iontophoresis-an approach for controlled drug delivery: a review. *Current drug delivery*, 4(1):1–10, 2007.

[7] José Juan Escobar-Chávez, Clara Luisa Domínguez-Delgado, and Isabel Marlen Rodríguez-Cruz. *Chemical and physical enhancers for transdermal drug delivery*. INTECH Open Access Publisher, 2012.

[8] J.A. Ferreira and M. Rente-Cabrita. Iontophoresis - estimating the released drug. *Proceedings of the 15th International Conference on Computational and Mathematical Methods in Science and Engineering, edited by J.Vigo-Aguiar*, pages 520–530, 2015.

[9] Mark S Gockenbach. *Partial differential equations: analytical and numerical methods*. Siam, 2010.

[10] Taís Gratieri and Yogeshvar N Kalia. Mathematical models to describe iontophoretic transport in vitro and in vivo and the effect of current application on the skin barrier. *Advanced drug delivery reviews*, 65(2):315–329, 2013.

[11] Tarja Jaskari, Marja Vuorio, Kyösti Kontturi, Arto Urtti, Jose A Manzanares, and Jouni Hirvonen. Controlled transdermal iontophoresis by ion-exchange fiber. *Journal of controlled release*, 67(2):179–190, 2000.

[12] Ajeet Kaushik, Rahul Dev Jayant, Vidya Sagar, and Madhavan Nair. The potential of magneto-electric nanocarriers for drug delivery. *Expert opinion on drug delivery*, 11(10):1635–1646, 2014.

[13] Azad Khan, Mohd Yasir, Mohd Asif, Iti Chauhan, Alok P Singh, Rajat Sharma, Pradeep Singh, and Shubham Rai. Iontophoretic drug delivery: History and applications. 2011.

[14] Stig Larsson and Vidar Thomée. *Partial differential equations with numerical methods*, volume 45. Springer Science & Business Media, 2008.

[15] Jeong W Lee, Jung-Hwan Park, and Mark R Prausnitz. Dissolving microneedles for transdermal drug delivery. *Biomaterials*, 29(13):2113–2124, 2008.

[16] Sarah A Molokhia, Yanhui Zhang, William I Higuchi, and S Kevin Li. Iontophoretic transport across a multiple membrane system. *Journal of pharmaceutical sciences*, 97(1):490–505, 2008.

[17] R Pignatello, M Fresta, and G Puglisi. Transdermal drug delivery by iontophoresis. i. fundamentals and theoretical aspects. *Journal of applied cosmetology*, 14(2):59–72, 1996.

[18] Giuseppe Pontrelli and Filippo de Monte. A two-phase two-layer model for transdermal drug delivery and percutaneous absorption. *Mathematical biosciences*, 257:96–103, 2014.

[19] Kakuji Tojo. Mathematical model of iontophoretic transdermal drug delivery. *Journal of Chemical Engineering of Japan*, 22(5):512–518, 1989.

[20] Martin L Yarmush, Alexander Golberg, Gregor Serša, Tadej Kotnik, and Damijan Miklavčič. Electroporation-based technologies for medicine: principles, applications, and challenges. *Biomedical Engineering*, 16(1):295, 2014.